Design and synthesis of Rho kinase inhibitors (I)

Atsuya Takami,[a,†] Masayuki Iwakubo,[a,†,‡] Yuji Okada,[a] Takehisa Kawata,[a]
Hideharu Odai,[b] Nobuaki Takahashi,[b] Kazutoshi Shindo,[a,§] Kaname Kimura,[a]
Yoshimichi Tagami,[a] Mika Miyake,[b] Kayoko Fukushima,[a] Masaki Inagaki,[c]
Mutsuki Amano,[d] Kozo Kaibuchi[d] and Hiroshi Iijima[a,*]

[a]Pharmaceutical Research Laboratories, Kirin Brewery Co. Ltd, 3 Miyhara-cho, Takasaki-shi, Gunma 370-1295, Japan
[b]Central Laboratory for Key Technology, Kirin Brewery Co. Ltd, 1-13-5 Fukuura, Kanazawa-ku, Yokohama,
Kanagawa 236-0004, Japan
[c]Laboratory of Biochemistry, Aichi Cancer Center Research Institute, 1-1 Kanokoden, Chikusa-ku, Nagoya, Aichi 464-8681, Japan
[d]Department of Cell Pharmacology, Nagoya University Graduate School of Medicine, 65 Maizuru-machi, Showa-ku,
Nagoya, Aichi 466-8500, Japan

Abstract—Several structurally unrelated scaffolds of the Rho kinase inhibitor were designed using pharmacophore information obtained from the results of a high-throughput screening and structural information from a homology model of Rho kinase. A docking simulation using the ligand-binding pocket of the Rho kinase model helped to comprehensively understand and to predict the structure–activity relationship of the inhibitors. This understanding was useful for developing new Rho kinase inhibitors of higher potency and selectivity. We identified several potent platforms for developing the Rho kinase inhibitors, namely, pyridine, 1*H*-indazole, isoquinoline, and phthalimide.
© 2004 Elsevier Ltd. All rights reserved.

1. Introduction

Cells sometime change their cytoskeletal structure in response to external stimulation. For example, an increase in the lysophosphatidic acid (LPA) concentration in plasma causes the contraction of the smooth muscle of blood vessels. This contraction was explained by the rearrangement of the cytoskeleton, which is a result of an intracellar signal response initiated by the LPA receptor at the cell surface that finally results in the phosphorylation of the myosin light chain. It is also known that such a cytoskeletal response is imperative for the cell adhesion process. Expression of the adhesion device such as integrin on the cell surface requires reorganization of the membrane proteins where actin plays an important role in the process.

Rho kinase,[1] which is also known as Rho-associated coiled-coil forming protein serine/threonine kinase (ROCK),[2] is one of the central regulatory molecules for cytoskeleton control and the cell adhesion process.[3] Rho kinase is activated by binding with the activated form of a low molecular weight G protein, Rho.[4] It will then phosphorylate myosin light chain and introduces the formation of stress fibers, adhesion cluster, and activation of adhesion devices on the cell surface. Rho kinase also phosphorylates myosin phosphatase, which catalyzes the dephosphorylation of the myosin light chain. The phosphorylated phosphatase is inactive. As a result, Rho kinase directly and indirectly enhances the phosphorylation of the myosin light chain.[5] It is interesting that contraction of the smooth muscle by the Rho pathway is independent from the Ca^{2+} pathway.[6]

Rho kinase is thought to play an important role in a variety of cellar functions such as stress fiber formation,

focal adhesion formation, cell aggregation, cell morphology, cytokinesis, cell migration, and Ca^{2+}-sensitization in the smooth muscle. Recent experiments have shown new functions of Rho kinase in cells, including centrosome positioning and cell-size regulation.[7a] More recently, it was shown that Rho kinase is involved in regulation of the amyloid precursor protein processing.[7b] Inhibitors of Rho kinase will be useful pharmaceutical candidates for a wide range of diseases such as hypertension, inflammation, cancer, and injury caused by ischemia and reperfuson.[8] Therefore, we have performed a screening of the Rho kinase inhibitors. Although any hit compounds did not indicate a high inhibition potential, the commonality of pharmacophores was observed among the hit compounds. Using this information and a Rho kinase homology model, a structure-based drug design was performed resulting in the successful generation of potent Rho kinase inhibitors of diverse scaffolds.

2. Screening of inhibitors

We identified 417 hit compounds as Rho kinase inhibitors by screening the in-house compound library (69,000 compounds). The first screening was based on an immobilized enzyme linked immunoassay. The hit compounds were then examined by enzyme kinetical assay employing [γ-^{32}P]-ATP and a synthetic peptide (S6 peptide). The inhibitors were classified into ATP-competitive, phosphate-acceptor-competitive, or other categories according to the inhibition mode. Figure 1 shows a few examples of the hit compounds. Most of the substrate-competitive inhibitors have high molecular weights and high hydrophillicity (**1**). These structures are contrary to the general understanding of drug-like compounds. On the other hand, the structures of inhibitors identified as ATP-competitive are drug-like
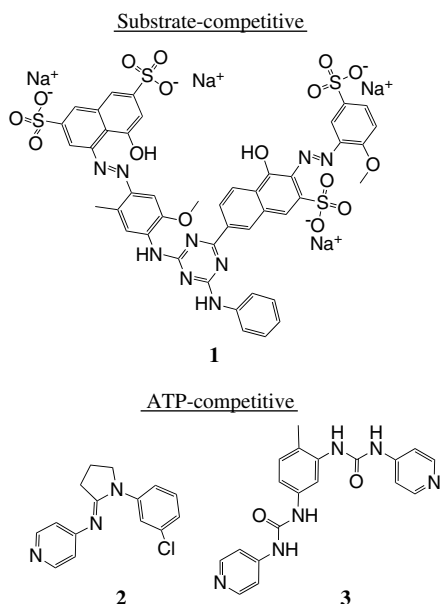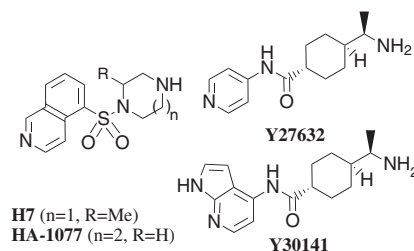
Figure 2. Known Rho kinase inhibitors.

(**2** and **3**).[9] Most of the ATP-competitive hits included one or more hydrogen bond accepter atoms. To our knowledge, the majority of potent low molecular weight kinase inhibitors reported so far are ATP-competitive and possess a hydrogen bond acceptor atom. It was also found that ATP-competitive hits are less hydrophilic than substrate-competitive ones, suggesting the possibility of good membrane permeability and absorption in vivo when administered. Therefore, we expected to identify suitable compounds to develop from the ATP-competitive hits.

However, none of the screening hits indicated a strong inhibitory activity ($IC_{50} > 3 \mu M$), while a standard inhibitor, HA-1077 (Fasdil) (Fig. 2),[10] indicated an IC_{50} of 0.1–0.3 μM. Furthermore, several cell based evaluations, in which the Rho kinase plays an important role, such as the formation of stress fibers in mouse 3T3 cells induced by LPA, aggregation of human B-cells by phorbol ester, and aggregation of human platelets were applied to the hit compounds. Here again HA-1077, the reference compound, exhibited a significant inhibition in these evaluations, while none of the screening hits exhibited clear and reproducible inhibitions for these assays.

3. Homology modeling and docking simulation

The crystal structure of a cAMP dependent protein kinase (cAPK) complexed with an inhibitor H7 (Fig. 2) was chosen as the template structure for homology modeling (Protein Data Bank[11] entry:1YDR[12]) because cAPK was very homologous to Rho kinase among the protein kinases whose three-dimensional structure are known (37% sequence identity). The amino acid sequence alignment of the Rho kinase and cAPK was made using the Needleman and Wunsch algorithm[13] (Fig. 3). The sequences of cyclin dependent protein kinase 2 (CDK2, PDB entry:1HCL[14]) and insulin receptor kinase (IRK, PDB entry:1IRK[15]) were also added to the alignment and their side-chain conformation were referred to build the homology model as described in the Experimental section.

The docking program used in this study, FlexiDock,[16] can contain defined rotatable bonds giving some flexibility to both the protein and the ligand, but the backbone conformation of the protein is fixed. Docking calculations of H7 and of ATP to the Rho kinase model were run as tests. Both reproduced the binding structures of H7 and ATP that were found in the complex

Figure 1. Example of hit compounds identified by screening Rho kinase inhibitors in the chemical library.

```
                                                  93
RHOK:  85                              EDYDVVKVIGRGAFGEVQLVRHKASQ----KVYAMKLLSKFEMIKRSDSAFFWEERDIMAFAN  143
CAPK:  15 VKEFLAKAKEDFLKKWENPAQNTAHLDQFERIKTLGTGSFGRVMLVKHMETG----NHYAMKILDKQKVVKLKQIEHTLNEKRILQAVN   99
CDK2:   1                 MENFQKVEKIGEGTYGVVYKARNKLTG----EVVALKKI-RLDTETEGVPSTAIREISLLKELN   59
IRK : 981         SSVFVPDEWEVSREK------ITLLRELGQGSFGMVYEGNARDIIKGEAETRVAVKTVNESASLRERIEFLNEASVMKGFTC 1056


                 167  171
RHOK: 144 SPWVVQLFCAFQDDKYLYMVMEYMPGGDLVNLMSNYD-----V------PEKWAKFYTAEVVLALDAIHSMGLIHRDVKPDNMLLDKHG  221
                                                                                  # #   #
CAPK: 100 FPFLVKLEFSFKDNSNLYMVMEYVAGGEMFSHLRRIG-----RF-----SEPHARFYAAQIVLTFEYLHSLDLIYRDLKPENLLIDQQG  178
CDK2:  60 HPNIVKLLDVIHTENKLYLVFEFLHQ-DLKKFMDASA----LTGI----PLPLIKSYLFQLLQGLAFCHSHRVLHRDLKPQNLLINTEG  139
IRK :1057 H-HVVRLLGVVSKGQPTLVVMELMAHGDLKSYLRSLRPEAENNPGRPPPTLQEMIQMAAEIADGMAYLNAKKFVHRDLAARNCMVAHDF 1144


          226
RHOK: 222 HLKLADFG-TCMKMDETGMVHCDTAVGTPDYISPEVLKSQGGDGYYGRECDWWSVGVFLFEMLVGDTPFYADSLVGTYSKIMDHKNSLC  309
          #*********************
CAPK: 179 YIQVTDFGFAKR-VKGRTWTLCGT----PEYLAPEIILSKG----YNKAVDWWALGVLIYEMAAGYPPFFADQPIQIYEKIVSGKVRFP  258
CDK2: 140 AIKLADFGLARA-FGVPVRTYTHE-VVTLWYRAPEILLGCKY---YSTAVDIWSLGCIFAEMVTRRALFPGDSEIDQLFRIFRTLGTPD  223
IRK :1145 TVKIGDFGMTRDIYETDYYRKGGKGLLPVRWMAPESLKDGV----FTTSSDMWSFGVVLWEITSLAEQPYQGLS--NEQVLKFVMDGGY 1227


RHOK: 310 FP---------------ED------------AEISKHAKNLICAFLTDREVRLGRNGVEEIKQHPFFKNDQWNWDNIRETAAPVVPE  369
CAPK: 259 SH---------------FS------------SDLKDLLRNLLQVDLTKRFGNL-KDGVNDIKNHKWFATTDWIAIYQRKVEAPFIPK  317
CDK2: 224 EVVWPGVTSMPDYKPSFPKWARQDFSKVVPPLDEDGRSLLSQMLHYDPNKRISAK----AALAHPFFQDVTKPVPHLRL*          298
IRK :1228 LD-----------QPDNCP-----------ERVTDLMRMCWQFNPKMRPTFL-EIVNLLKDDLH-PSFPEVSFFHSEENK*         1283


          382
RHOK: 370 LSSDIDSSNFDDIEDDKGDVETFPIPKAFVGNQ*                                                        402
CAPK: 318 FKGPGDTSNFDDYEEEEIRVSINEKCGKEFSEF*                                                        350
```

Figure 3. Sequence alignment of human Rho kinase with bovine cAMP dependent protein kinase (PDB:1YDR), human insulin receptor kinase (PDB:1IRK), and human cyclin dependent protein kinase 2 (PDB:1HCL). Sequences of the reference kinases were ones described in Protein Data Bank. Secondary structures defined in the crystal coordinates data are marked by wavy underlines for β-sheets and by double underlines for α-helices. The activation loop is marked with asterisks. Conserved catalytic residues were indicated by '#'. Residues that define the ligand-binding site of the Rho kinase are underlined.

with cAPK and CDK2, respectively. However, another test run employing staurosporin as a ligand was a failure because FlexiDock could not handle a conformational change in the backbone structure. It was shown that the shape of the ligand-binding pocket was wide-open in the crystal structure of the staurosporin–cAPK complex (PDB entry:1STC)[17] in order to accommodate the large ligand molecule.

It should be noted that the template cAPK structure is the activated form and phosphorylated in the activation loop. The activation loop positions outward from the ligand-binding pocket. Recently, it was reported that designing an inhibitor that binds to both inactive and activated conformations of the kinase is advantageous for enhancing the kinase specificity.[18] In this study, however, the homology model of Rho kinase based on the activated cAPK was employed because reliable modeling of the inactive conformation of the activation loop is not possible. It should be noted that the recombinant Rho kinase used in this study lacked the C-terminal regulatory subunits and was constitutively active.[19] The design and experiments in this study are under these limitations.
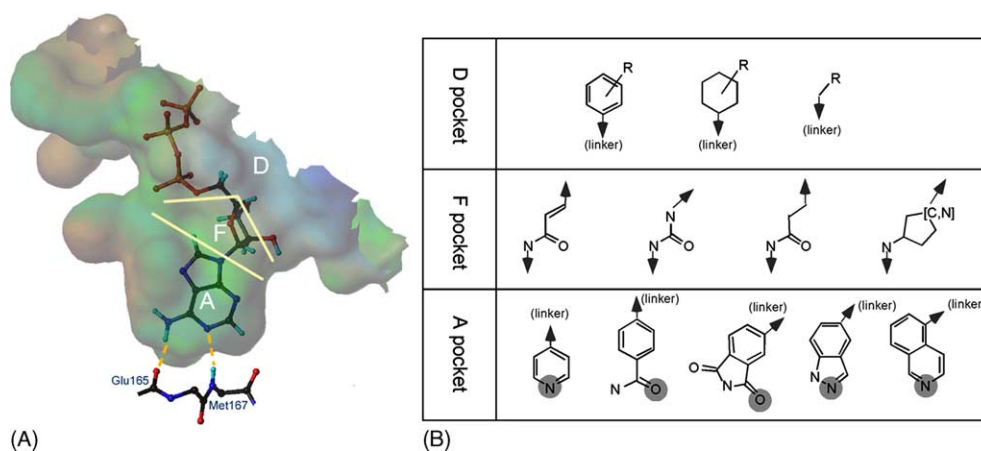
4. Ligand-binding pocket

The ligand-binding pocket could be divided into three regions (Fig. 4A). The bottom of the pocket is flat in shape and hydrophobic (A region). Characteristic is the existence of an important hydrogen bond donor site present in the backbone NH of Met167. This site is utilized to form a hydrogen bond with the N1 nitrogen atom of the adenine ring of ATP. This hydrogen bond is found in a number of protein kinase–inhibitor complex structures reported to date and is considered to be fundamental for the intermolecular interaction between protein kinases and inhibitors. The second region of the pocket is above the adenine region (F region). This region is spherical in shape and also hydrophobic. This region accepts the furanose ring of ATP. The third region (D region) is formed by residues, Ile93:Arg95, Ala97:Gly99, Gly170:Leu172, Asp209:Asn214, and Asp227:Phe228. This distal region is open to the molecular surface of the enzyme. A part of the nucleotide-binding loop also contributes to determining the shape of the D pocket.

Comparison of the shapes of the ligand-binding pockets of the Rho kinase and the cAPK indicated that the F region of the Rho kinase is wider than that of the cAPK. This difference could be explained by the amino acids Ile95 and Ala226, which correspond to Leu47 and Thr183 of cAPK, respectively. The D region of the Rho kinase is wider than that of the cAPK. This is also explained by the amino acid replacements to smaller ones. Glu127 and Tyr330 of cAPK were replaced by Asp171 and Ile382 in the Rho kinase model. The shape of the A region is very similar.

5. Design of inhibitors

Pyridine derivatives with substitution at the 4-position such as compounds **2** and **3** (Fig. 1) were representative

Figure 4. (A) Ligand-binding pocket of Rho kinase homology model. The pocket was visualized by the channel surface representation calculated by the Connolly module available in the SYBYL software package.[26] The surface was colored by lipophilicity; brown > green > blue. A docking model of ATP is shown. Hydrogen bonds between N1of ATP and HN of Met167, and the amino group at the 6-position and C=O of Glu165 are indicated as dashed lines. The pocket was partitioned into three parts; adenine region: A, franose region: F, and distal region: D. (B) Chemical substructures designated for each division of the ligand-binding pocket. Arrows indicate attachment of fragments. Hatched circles indicate possible hydrogen bond acceptor atom.

screening hits, though their inhibitory potencies were low. A docking model of **2** (Fig. 5A) suggested that the aromatic pyridine ring would fit into the A region and would be stabilized by a hydrogen bond between the pyridine nitrogen atom and the backbone NH of Met167. Based on the facts that **2** is an ATP-competitive inhibitor and that the existence of a hydrogen bond between an inhibitor and kinase at the bottom of the A region is observed in many inhibitor–kinase complex structures, we assumed that an aromatic ring and a

nitrogen atom of the aromatic ring are essential pharmacophores of Rho kinase inhibitors.

The docking model proposed several hypotheses for inhibitor design. First, molecular fragments that have a hydrogen acceptor and that are planar would fit the shape of the A region. For example, one six-member aromatic ring or fused 6–6 or 6–5 ring were candidate substructures for the A region. Second, as the furanose region (the F region) is relatively spacious, many
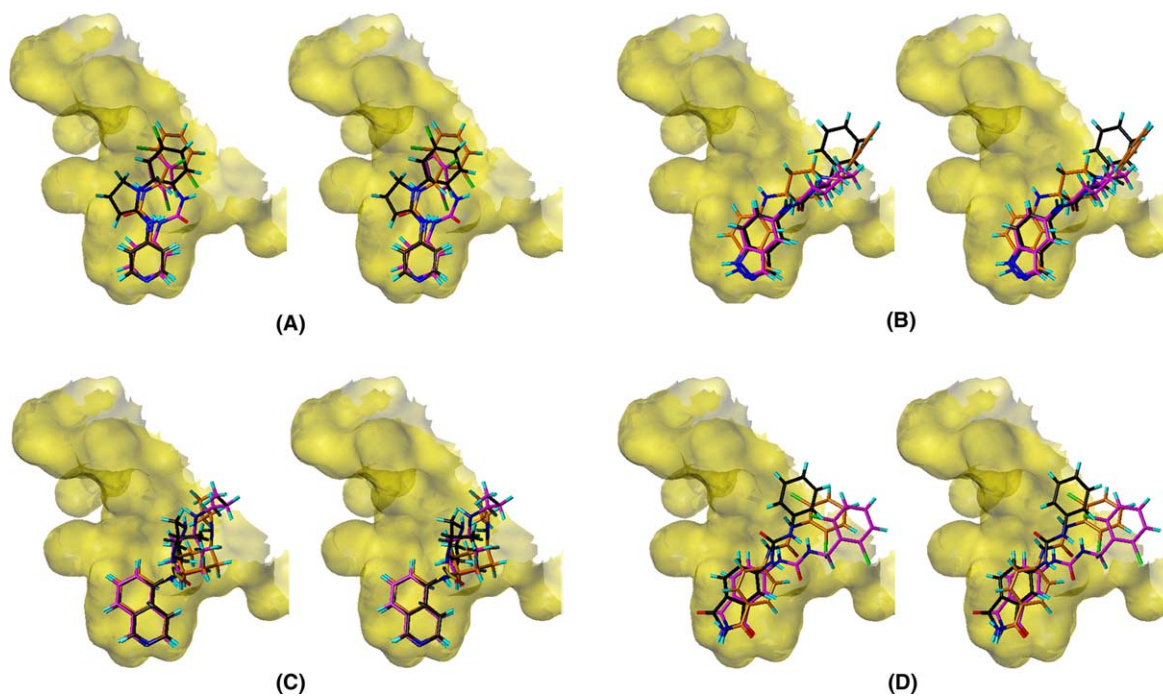
Figure 5. Docking models of Rho kinase inhibitors (stereo view). (A) Pyridine derivatives: **2** (carbon atoms colored in black), **4b** (magenta), and **5a** (orange). (B) Indazole derivatives: **12a** (carbon atoms colored in magenta), **14b** (black), and **20b** (orange). (C) Isoquinoline derivatives: **22c** in equatorial conformation (carbon atoms colored in orange), **22c** in axial conformation (magenta), and H7 (black). (D) phthalimide derivatives and benzamide: **29c** (carbon atoms colored in magenta), **30c** (black), and **31** (orange).

chemical substructures could be applied to this region of the pocket. Third, the top part of the pocket (the D region) is cleft-like in shape and a wide range of chemical fragments would fit this cleft. Fourth, a substructure for the furanose region could be considered as a linker to join an aromatic substructure for the A region and a substructure for the D region. Figure 4B shows examples of the designed substructures for each region. We built virtual inhibitors by combination of the substructures and then those virtual compounds were submitted to the docking simulations. The resulted docking models were interactively examined with the aid of computer graphics.

6. Pyridine scaffold

Pyridine derivatives that provide a linker moiety at the 4-position gave good docking models. Especially, linkers that are planar in shape were good (Fig. 5A). Table 1 shows such examples (4a, 4b, 5a, 6a, and 6b) that exhibited IC_{50} values of 0.2–0.9 μM. In contrast, pyridine derivatives with linker substitution at the 3-position failed to give docking models that retained the essential hydrogen bond. 3-Substitued pyridine derivatives existed in the screening library and none indicated inhibitory activity (data not shown).
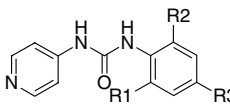
The 2,6-dichlorophenyl group was a good substructure fragment for phenylurea and benzylurea derivatives (4b and 5a) than a free phenyl group (4e and 5d), although the roles of the 2,6-dichlorophenyl group of 4b and 5a in the ligand-binding pocket are different (Fig. 5A). The dichlorophenyl group of 4b occupied the F region from wall to wall in the docking model, while the dichlorophenyl group of 5a occupied the cleft of the D region, allowing many types of substitutions (5b–f). Removal of one chlorine atom from 4b drastically reduced the inhibitory activity (4d) while a derivative lacking a chlorine atom from 5a retained its inhibitory potency (5c). The structure–activity relationship of the 4b derivatives clearly indicated that 2,6-dichloro substitutions is crucial (4a–c). Compound 4e exhibited no inhibition while 5d retained the potency, indicating that full use of the F region is important for 4b to interact with the enzyme. This hypothesis was further supported by the recovery of inhibitory activity found in 4f and 4g.
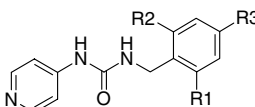
In the docking models of 4b and 5a, the urea bonds were cis and in plane with the pyridine ring. Indeed, the screening hit 2 could be considered as a conformationally restrained cis urea derivative. The fact that N-methylation abolished the inhibitory potency (8) would support the importance of the conformation of urea.

Because the A region is wide enough to contain both the pyridine ring and a part of the linker moiety, the aromatic ring and the linker must be in the same plane. Derivatives that include methylene (CH_2) in the attachment at the 4-position (9a and 9b) were not inhibitory and in good accordance with the fact that no good docking model was obtained for these molecules. On the other hand, derivatives that had a planar linker
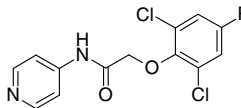
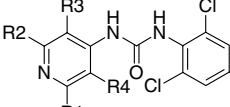**Table 1.** Inhibitory potencies of pyridine derivatives

entry	IC50 (μM)	R1	R2	R3
4a	0.2	Cl	Cl	Cl
4b	0.9	Cl	Cl	H
4c	>10	Cl	H	Cl
4d	>10	Cl	H	H
4e	>10	H	H	H
4f	2.0	F	F	H
4g	13.6	CF$_3$	F	H
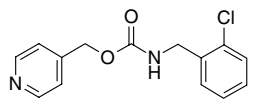
entry	IC50 (μM)	R1	R2	R3
5a	0.8	Cl	Cl	H
5b	4.1	Cl	H	Cl
5c	7.2	Cl	H	H
5d	10.2	H	H	H
5e	7.0	F	F	H
5f	2.2	CF$_3$	F	H
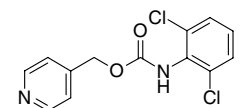
entry	IC50 (μM)	R
6a	0.5	F
6b	0.9	H
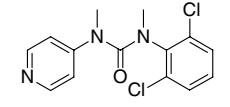
entry	IC50 (μM)	R1	R2	R3	R4
7a	>10	H	H	H	NH$_2$
7b	>10	H	H	Cl	Cl
7c	>10	Cl	Cl	H	H
7d	>10	Cl	H	H	H
7e	>10	NH$_2$	H	H	H
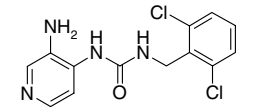
entry	IC50 (μM)
9a	>10
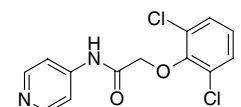
entry	IC50 (μM)
9b	>10

entry	IC50 (μM)
8	>10

entry	IC50 (μM)
10	>10

entry	IC50 (μM)
11	>10

(**6a** and **6b**) were good ligands in the docking simulation and were experimentally proven inhibitory. A known Rho kinase inhibitor, Y27632 (Fig. 2), could be considered to belong to this family. Co-planarity between the linker and the pyridine ring was decisive for the pyridine derivatives.

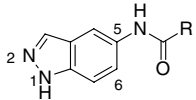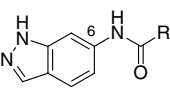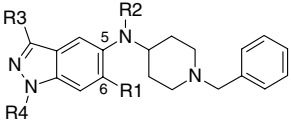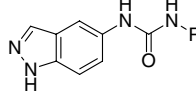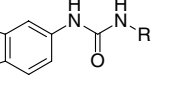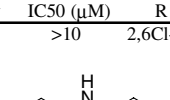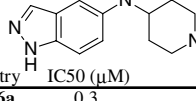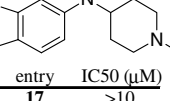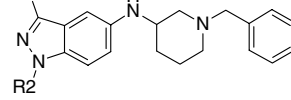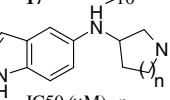As the A region is spacious enough for a pyridine ring, introduction of substitution might be possible. In fact, a higher affinity of Y30141 (K_i 0.3 μM) than Y27632 (K_i 0.05 μM) to Rho kinase was reported.[20] This could be explained by the full occupancy of the A region and/or by formation of the additional hydrogen bond to the C=O of Glu165 by the docking model. Thus the effect of substitutions at the 2- or 3-position of the pyridine rings were investigated. Introducing the substitutions to the 3-position of the pyridine ring of **4b** and **5a** reduced the inhibitory activity. Conformational analyses of the 3-substituted pyridine indicated that the substitutions would destabilize the active conformation in which the pyridine ring and urea linker is co-planar (**7a**, **7b**, and **10**) due to a steric interference with the linker urea group. Substitutions at the 2-position were unfavorable because they would orient toward the bottom wall of the A region and cause unfavorable contact between the inhibitor and the enzyme (**7c**, **7d**, and **11**). Introduction of an amino group (hydrogen bond donor) at the 2-position was intended to form an additional hydrogen bond with C=O of Glu165, but this was not effective (**7e**). The docking model of **4b** suggested that the use of the urea linker would strictly determine the positioning of the pyridine ring in the A region, which would not allow placement of the amino group of **7e** at the proper distance from the C=O of Glu165.

7. 1*H*-Indazole scaffold

The 1*H*-indazole scaffold has a five-membered ring system with a hydrogen bond acceptor atom at the 2-position. Docking models suggested that the A region could be better occupied by the indazole ring since the indazole moiety is larger in size than the pyridine ring system (Fig. 5B). There are two possible positions to attach a linker substructure. Docking of the 5-substituted and 6-s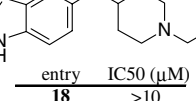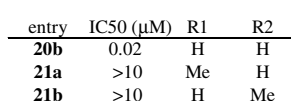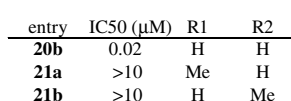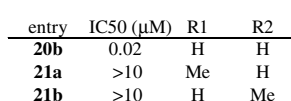ubstituited analogues to the Rho kinase model are both possible. The difference between the two analogues was that an interaction between NH at the 1-position of indazole and C=O of Glu165 is possible for the 5-substituted analogue in addition to the essential hydrogen bond between N-2 of indazole and NH of Met-167. The docking model of the 6-substituted analogues with two hydrogen bonds was not possible, because there was no space available to the linker and the peripheral moiety given that the indazole ring was placed in the A region in the same manner allowed for the 5-substituted analogues. An enzyme inhibition study revealed that the 5-substituted analogues exhibited a distinctively higher potency than those with the linker substitution at the 6-position (**12a** vs **13a**, **12b** vs **13b**, **12c** vs **13c**, **14a** vs **15**, **16b** vs **17**, Table 2).
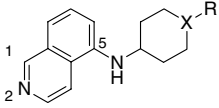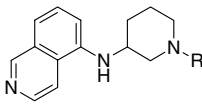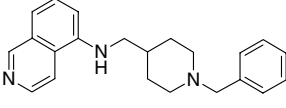
The absence of N-2 lead to the loss of inhibitory potency, confirming the importance of the essential hydrogen bond (**18**). If the additional hydrogen bond between the NH-1 and C=O of Glu165 proposed by the docking study existed, a substitution at the 3-position should cause an unfavorable steric interaction with Tyr166. Such an analogue (**19e** and **21a**) indeed lost the potency. Alkylation of N1, which disables the formation

Table 2. Inhibitory potencies of 1*H*-indazole derivatives
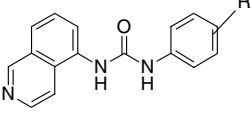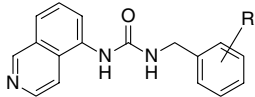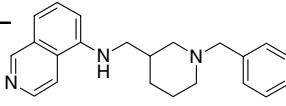
entry	IC50 (μM)	R
12a	0.5	cycloHex
12b	0.9	CH₂-cycloHex
12c	0.5	CH₂-O-(2,6Cl,4F-Ph)

entry	IC50 (μM)	R
13a	>10	cycloHex
13b	>10	CH₂-cycloHex
13c	>10	CH₂-O-(2,6Cl,4F-Ph)

entry	IC50 (μM)	R1	R2	R3	R4
16c	0.2	H	H	H	H
19a	0.4	F	H	H	H
19b	>10	OMe	H	H	H
19c	>10	H	(CO)Me	H	H
19d	>10	H	Et	H	H
19e	>10	H	H	Me	H
19f	>10	H	H	H	Me

entry	IC50 (μM)	R
14a	1	2,6Cl-Ph
14b	0.3	CH₂-Ph

entry	IC50 (μM)	R
15	>10	2,6Cl-Ph

entry	IC50 (μM)	R
16a	0.3	H
16b	0.7	Et
16c	0.2	CH₂-Ph

entry	IC50 (μM)
17	>10

entry	IC50 (μM)	R1	R2
20b	0.02	H	H
21a	>10	Me	H
21b	>10	H	Me

entry	IC50 (μM)	n	R
20a	0.8	2	nPr
20b	0.02	2	CH₂-Ph
20c	0.1	1	H
20d	0.03	1	CH₂-Ph

entry	IC50 (μM)
18	>10

Table 3. Inhibitory potencies of isoquinoline derivatives

entry	IC50(μM)	X	R
22a	0.1	N	CH$_2$Ph
22b	0.3	N	nPr
22c	0.1	CH	NH-nPr
22d	0.2	CH	NHMe

entry	IC50(μM)	R
23a	0.2	CH$_2$Ph
23b	0.1	(CH$_2$)$_3$CH(Me)$_2$

entry	IC50(μM)
26	>10

entry	IC50(μM)
27	>10

entry	IC50(μM)	R
24a	>10	4-(CO)Me
24b	>10	2,6-Cl
24c	>10	2,4,6-Cl

entry	IC50(μM)	R
25a	>10	2,6-F
25b	>10	2,6-Cl

entry	IC50(μM)
28	>10

of the additional hydrogen bond, also resulted in the loss of inhibitory potency (**19f** and **21b**). Taken together, the additional hydrogen bond would exist and it is an important pharmacophore of the 5-substituted indazole derivatives.

As shown in Table 2, a variety of linker choices were allowed for the 5-substituted indazole scaffold (e.g., **12a–c**, **14a–b**, **16a–c**, and **20a–d**). In contrast to the pyridine scaffold, a saturated ring system could be used as a linker substructure in addition to the amide and urea substructures. A modeling study indicated that the planar linkers such as the amide or urea moieties position its plane orthogonal to the indazole ring to fill the spherical F region and that the piperidine ring could effectively fill the F region. See the docking model of **12a**, **14b**, and **20b** in Figure 5B. Depending on the choice of linker, the indazole ring orients differently in the A region of the ligand-binding pocket. This observation suggests that the indazole derivatives would differ in kinase specificity spectra based on the choice of the linker moiety.

N-alkylation of the linker nitrogen atom of **16c** decreased the inhibitory potency since no more space is available for the alkyl group in the F region (**19c** and **19d**). A large substitution at the 6-position of **16c** decreased the inhibitory potency (**19b**) while a smaller substitution (**19a**) did not. This fact also suggests the full occupation of the F region by indazole derivatives that have an aminopiperidine as a linker substructure. In fact, derivatives that have a cyclic aliphatic ring as the linker substructure exhibited a higher potencies (**20a–d**) than derivatives with the amide or urea linkers.

8. Isoquinoline scaffold
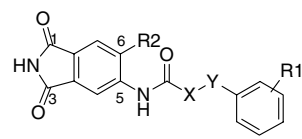
The isoquinoline scaffold with substitution at the 5-position could be considered compatible with the pyridine scaffold with a co-planar linker at the 4-position. HA-1077 (Fig. 2) belongs to this category. As the isoquin-

oline ring is planar, a planar linker is no longer necessary. Here an amine nitrogen atom and a saturated ring play a key role as the linker fragment (**22a–d**, **23a**, and **23b**, Table 3). Compound **22c**, whose docking model is shown in Figure 5C, is an example of a simple isoquinoline inhibitor. Note that both the axial and equatorial conformations were possible for the bond that links the saturated ring and the nitrogen atom attached to C5. The *syn*- and *anti*-isomers of **22c** were equally potent (IC$_{50}$=0.1 μM), suggesting that the orientation of the propyl group in the D region is not crucial. The X-ray structure of H7[11] and the docking model of **22c** are shown in Figure 5C.

Employment of the isoquinoline scaffold would restrict the choice of the linker substructures. A docking study of compounds that include the urea linker (**24a–c**, **25a**, and **25b**), an analogue with an insertion of a CH$_2$ group between N5 and a saturated ring (**26** and **27**) or replacing the saturated ring with a planar aromatic ring (**28**) indicated that these inactive derivatives did not allow proper use of the F region.
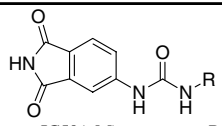
9. Phthalimide scaffold

Phthalimide is a flat aromatic 5–6 ring system and has hydrogen acceptors that are not included in the ring system. As shown in Figure 4A, the essential hydrogen bond donor (HN of Met167) is located off-center on the bottom of the A region. Thus phthalimide was considered to utilize the A region of the ligand-binding pocket in a different way. The structure–activity relationship of the phthalimide analogues is summarized in Table 4. Compounds with a urea linker showed an inhibitory potential (**29a–d**, and **30a–c**). Figure 5D shows the docking model of **29c** and **30c**. In addition to the essential hydrogen bond between C=O at the 3-position of the ligand and NH of Met167, NH of phthalimide formed a hydrogen bond with C=O of Glu165. Another carbonyl group at the 1-position was not utilized to form a hydrogen bond.

Table 4. Inhibitory potencies of phthalimide derivatives

entry	IC50(μM)	X	Y	R1	R2
29a	0.4	NH	CH_2		H
29b	0.3	NH	CH_2	2-Cl	H
29c	0.1	NH	CH_2	2,6-Cl	H
29d	0.1	NH	CH_2	2,6-Cl	Cl
29e	>10	O	CH_2	2,6-Cl	
29f	>10	CH_2	O	2,6-Cl	H

entry	IC50(μM)	R
30a	8.3	nPr
30b	0.9	Ph
30c	1.9	2,6-Cl-Ph
30d	>10	
30e	>10	

entry	IC50(μM)
31	9

Analogues with an amide moiety as the linker were not potent (**29e** and **29f**). As far as using the urea linker, the hydrophobic group for the D region should be aromatic (**30d** and **30e**). Introduction of a chlorine atom at the 6-position (**29d**) did not abolish the inhibitory potential of **29c** being in agreement with a molecular mechanical calculation that the urea conformation (torsion angle of C6–C5–N^{linker}–C^{linker}=−175°) found in the docking model of **29c** would not be destabilized by the substitution at the 6-position by a chlorine atom.

It was shown that the hydrogen bond acceptor of the inhibitor should not necessarily be included in an aromatic ring system. We then investigated the benzamide scaffold as an open form of the phthalimide scaffold. The docking simulation of **31** gave a reasonable docking model that is similar to the binding model of the phthalimide inhibitors (Fig. 5D). However, the inhibi-

tory potency was low for this scaffold. From 21 synthesized benzamide derivatives, only the compound **31** exhibited an IC$_{50}$ value less than 10 μM, while the structurally 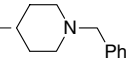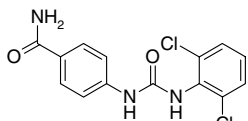corresponding phthalimide **30c** exhibited an IC$_{50}$ value of 1.9 μM. This fact suggests that the hydrophobic occupancy of the A region is very important. It should be noted in the known crystal structures of benzamides, the formylamide moiety is not co-planar with the phenyl ring (dihedral plane angle approx. 20–30°),[21] suggesting that the planarity of the hydrophobic group is also important.

10. The characterization of inhibitors

Several Rho kinase inhibitors were tested for their selectivity for other kinases such as MAP kinase, cAMP dependent protein kinase, protein kinase C, and some receptor tyrosine kinases. Table 5 shows the results, indicating that the inhibitors designed in this study indicated specificity to the Rho kinase and ATP-competitive (Fig. 6).

11. Conclusion

A high-throughput screening was carried out to discover Rho kinase inhibitors. Based on a docking model of screening hit compounds with a homolog model of Rho kinase, a synthetically feasible virtual library shown in Figure 4B was designed. With the aide of docking simulation, we selected possible active structures as well as possible inactive structures from the virtual library. A few of each of the possible active and the possible inactive compounds were synthesized and submitted for biological assessments. If the result was in accordance with the docking simulation, we inferred that we obtained an experimentally proven docking model. Designing derivatives of the active compounds was then a rather easy and safe task. Although accuracy or reliability of a homology model is not easy to be evaluated, Bossemeyer and co-workers experimentally demonstrated that the cAPK crystal structure would be a reliable template for homology modeling of the AGC protein kinase family.[28] Rho kinase belongs to the AGC protein kinase family. We believe that our homology model was a reliable one. This study demonstrated that docking simulation with a structure of the target protein is a robust method to explore a wider chemical space with a smaller number of compounds.

Table 5. Specificity of inhibitors (IC$_{50}$ in μM)

Entry	Rho kinase	MAP kinase	cAMP dependent protein kinase	PKC	PDFG–R kinase	SCF–R kinase
4a	0.20	>30	>10	>10	>10	>10
5a	0.77	>30	>10	>10	>10	>10
6a	0.48	>30	>10	>10	>10	>10
12c	0.46	>30	>10	>10	>10	>10
29c	0.11	>30	>10	10% @ 10 μM	>10	>10
H-1077	0.15	>30	76% @ 10 μM	17% @ 10 μM	>10	>10
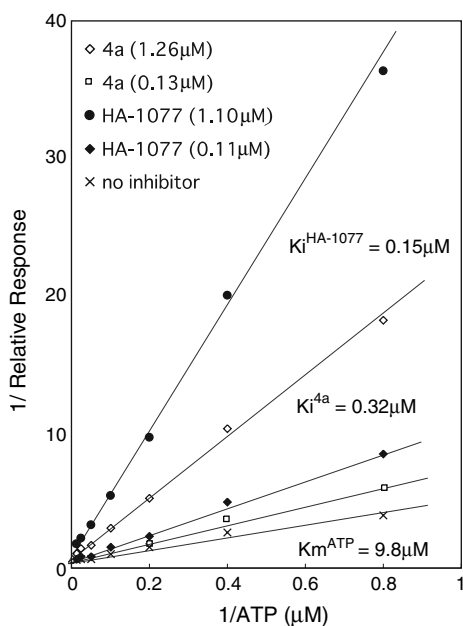
Figure 6. Lineweaver–Burk plot for **4a**. K_i value for HA-1077 was comparative with those previously reported.[6,27]

The existence of a hydrogen bond acceptor and the presence of an aromatic ring of a suitable size were important for an inhibitor to interact with the A region of the ligand-binding pocket. The combination of the substructures for the A region and the F region would determine the potency of the inhibitor and the enzyme selectivity.

It was also shown that different scaffolds were possible as lead structures for the Rho kinase inhibitors. We succeeded to design and synthesize novel lead compounds. The optimization process and structure–activity relationship of these lead scaffolds found in this study will be reported elsewhere.

12. Experimental

Commonly used abbreviations; DMF (dimethylformamide), EtOAc (ethyl acetate), EtOH (ethanol), MeOH (methanol), ATP (adenosine triphosphate), DMSO (dimethylsulfoxide), Ph (phenyl group), Me (methyl group), Et (ethyl group), nPr (normal propyl group), cycloHex (cyclohexyl group), WSC–HCl (1-ethyl-3-(3-dimethylaminopyropyl)carbodiimide hydrochloride), HOBt–H_2O (5-hydroxybenzotriazole mono hydrate), PDGF (platelet derived growth factor), SCF (stem cell factor), ELISA (enzyme linked immunoadsorbent assay).

12.1. High-throughput screening

Enzyme and substrate: The catalytic domain of the bovine Rho kinase was expressed as the GST (glutathione-*S*-transferase) fusion protein in insect cells (Sf9) using bacullovirus and purified by employing glutathi-

one affinity chromatography.[22] The GST fusion protein of the head domain of glial fibrillary acidic protein (GFAP) was expressed in *E. coli*, purified by glutathione affinity chromatography and used as a substrate (phosphate acceptor).[23]

Fixing GFAP on microplates: A 100 μL aliquot of GFAP solution (0.1 mg/mL) was added to each well of 96-well ELISA plates and the plates were kept at 4 °C overnight. The plates were washed three times with PBS (100 mM sodium phosphate, pH 7.4), then 250 μL of blocking buffer solution (5% bovine serum albumin, 5% sucrose in 10 mM sodium phosphate buffer of pH 8.0) was added and stored at 4 °C overnight. The blocking buffer was removed by suction and the wells were washed with PBS.

Kinase reaction: Each 100 μL of the reaction buffer (50 mM Tris–HCl buffer pH 7.5, 5 mM $MgCl_2$, 1 mM EDTA, 10 μM ATP) was added to the wells. Test compounds (1 mg/mL DMSO) were added to a final concentration of 10 μg/mL. The enzyme reaction was started by adding recombinant Rho kinase (final 5 μg/mL). The reaction was carried out for 2 h at rt.

The amount of phophorylated GFAP was determined by the ELISA method. Microplates were washed three times with PBS. The monoclonal antibody KT13 (mouse monoclonal antibody specific to phosphorylated GFAP)[23] was added and stored at rt for 1 h. The wells were washed five times with PBS followed by adding the secondary antibody (goat anti-mouse IgG antibody conjugated with horse radish peroxidase, Biorad 172-1011). After 1 h, the wells were washed seven times with PBS. The peroxidase activity was then measured by adding 100 μL of peroxidase reaction solution (prepared freshly with *o*-phenylenediamine 13 mg, 1.63 mL MeOH, 30.88 mL H_2O, and concd H_2O_2 11 μL). The reaction was stopped by adding 100 μL of 2 N H_2SO_4. Absorbance at 490 nm was measured.

12.2. Rho kinase inhibitory activity

The test compounds (10 μL, DMSO solution) were added to the reaction buffer (Tris–HCl buffer 100 mM, pH 7.5, containing $MgCl_2$ 10 mM, EGTA 2 mM, and EDTA 2 mM, total volume 100 μL). Ribosomal S6 kinase substrate (S6 231–239 peptide, CarbioChem, final concentration 1 μM) was used as the substrate. The enzymatic reaction was initiated by adding the recombinant Rho kinase together with ATP ([γ-^{32}P]-ATP, final concentration 10 μM). The reaction was carried out at 30 °C and terminated by adding 50 μL of 150 mM phosphoric acid. Reaction solution (40 μL) was adsorbed on a strip of filter paper (Whatman P81 ion-exchange chromatography paper). The strips were briefly dried and transferred to a conical flask filled with an excess amount of phosphoric acid solution (75 mM) and radioactive ATP was washed away from the strips. This operation was repeated three times followed by a rinse with water. The amount of the phosphorylated substrate was measured by a liquid scintillation counter (Wallac 1205 Beta Plate).

12.3. P42-mitogen activated protein kinase (MAP kinase-2) assay

The effect of compounds on the MAP kinase activity was examined using the in vitro kinase assay. Myelin basic protein (MBP) was used as a kinase substrate and 6 µg of MBP was incubated in 30 µL of buffer containing 18 mM HEPES (pH 7.4), 10 mM $MgCl_2$, 1 mM vanadate, 5 mM NaF, 1 mM β-glycerophosphate, 1 mM EDTA, 20 µM $[\gamma\text{-}^{32}P]$-ATP (5 µCi), and 0.2 µg of purified activated GST-p42 MAP kinase (UBI) at 30 °C for 30 min in the presence or absence of compounds. The proteins were then transferred onto P81 ion-exchange chromatography papers (Whatman) and washed three times with 75 mM phosphoric acid followed by a rinse with water. The radioactivity of the proteins was measured using a liquid scintillation counter.

12.4. cAMP dependent protein kinase assay

The catalytic subunit of bovine heart cAMP dependent protein kinase (PKA) was purchased from Pierce. The phosphorylation reaction was determined using the fluorescence intensity quenching method with a fluorophore-labeled kemptide as the substrate (IQ™ kinase reagent from Pierce). The assay buffer contained 20 mM Tris–HCl (pH 7.2), 10 mM $MgCl_2$, 2 mM ATP, 0.012% Triton X-100, 60 µM labeled kemptide peptide and inhibitor in a total volume of 30 µL. Fifteen units of the enzyme was added and incubated at rt for 20 min. The inhibitor was added as a DMSO solution. The final concentration of the DMSO was less than 10%.

12.5. Protein kinase C inhibitory assay

Rat brain PKC was purchased from Sigma. Biotylnylated myelin basic protein peptide (Calbiochem) was used as the substrate. The assay buffer contained 20 mM Tris–HCl (pH 7.5), 10 mM $MgCl_2$, 0.5 mM $CaCl_2$, 15 µM $[\gamma\text{-}^{32}P]$-ATP (25 µCi), 0.03% Triton X-100, 300 µg/mL of phosphatidyl-L-serine, and 30 µg/mL of 1,3-diolein (diacylglycerol), 25 µM peptide, and inhibitor in a total volume of 20 µL. The reaction was started by the addition of PKC (25 mU, 5 µL). The reaction was stopped by the addition of 10 µL of 8 M guanidine hydrochloride. The phosphorylated peptide was recovered as Avidin complex by using a PKC assay kit supplied by Calbiochem. The inhibitor was added as a DMSO solution. The final concentration of the DMSO was 10%.

12.6. Receptor tyrosine kinase assay

The effects of compounds on PDGFR-β and c-Kit kinase activities were measured using sandwich ELISAs. NIH3T3 and KU812F cells were used for the PDGFR-β and the c-Kit assay, respectively. Serum starved cells were treated with or without compounds at 30 °C for 30 min. NIH3T3 cells and KU812F cells were then stimulated with 50 ng/mL PDGF-bb for 5 min and 100 ng/mL SCF for 15 min at 37 °C, respectively. The cells were lysed with HNTG [20 mM HEPES (pH 7.5), 150 mM NaCl, 0.2% Triton X-100, 10% glycerol, 5 mM Na_3VO_4, 2 mM $Na_4P_2O_7$, and 5 mM EDTA] and transferred to 96-well ELISA plate pre-coated with anti-phosphotyrosine antibody, PY20 (BD. Bioscience), and incubated at rt for 1 h. After washing, the anti-PDGFR-β antibody (Santa Cruz) or the anti-c-Kit polyclonal antibody (Santa Curz) was added to the well and incubated at rt for 1 h. The receptor–antibody complex was probed with horseradish peroxidase conjugated anti-rabbit-IgG antibody (Amersham) and the color developed with TMBZ (Sumitomo Bakelite).

12.7. Homology modeling of Rho kinase catalytic domain

A crystal structure of cAMP dependent protein kinase (a protein kinase A, cAPK) solved by Bossemeyer and co-workers was chosen as the template structure (Protein Data Bank entry:1YDR).[12] The sequence of cyclin dependent protein kinase 2 (CDK2: Protein Data Bank entry:1HCL)[14] and the insulin receptor kinase (IRK: Protein Data Bank entry:1IRK)[15] were also aligned to help the side-chain modeling as described below (Fig. 3).

First, the insertion/deletion was adjusted. There were four loops where such an adjustment was required. Four-residue insertion occurs in the flexible activation loop (Phe228:Pro249 in Rho kinase sequence corresponding to Phe185:Pro202 of cAPK). Considering that the conformation of the activation loop is not conserved among the protein kinases whose three-dimensional structures were known, we dare not model this loop and left it as of cAPK. Thus our homology model is a chimerical model. Except for the activation loop, the other insertion/deletion patches (one-residue deletion between Gly136 and Ser139 of cAPK, four-residue insertion between Gly214 and Tyr215 of cAPK and one-residue insertion between Leu284 and Lys285 of cAPK) were modeled by the loop search program available in the SYBYL BIOPLYMER module. Since there were no further insertion/deletions except the loops, the backbone atom coordinates of the rest of the template protein were not modified.

Second, the amino acid residues of cAPK were altered according to the sequence of the Rho kinase. The side-chain conformation was determined by the following rules.

(1) If an amino acid residue was identical between Rho kinase and the temperate cAPK, the side-chain conformation found in the cAPK structure was preserved for the residue. Replacement of any amino acid to Ala or Gly was accomplished by simply shortening the side chain of a cAPK residue.

(2) If amino acid replacement was 'similar' or 'smaller', for example, replacement Ile with Val, Thr with Val, Lys with Arg, replacing an aromatic amino acid residue with aromatic one, replacing an amidic residue with the

corresponding acidic one (replacing Asn to Asp, Gln to Glu), etc., the χ torsion angles of the cAPK side chain were copied to the replaced residue. Replacing Asn115 of cAPK to Tyr159 belongs to this category by treating the aromatic ring as an equivalent of the plane defined by the amide group of the asparaginyl residue. Mutating an acidic amino acid to its corresponding neutral residue was carried out by considering the formation of hydrogen bonds or favorable electrostatic interactions to locate the carbonyl and amide groups. Similarly, an aromatic residue was converted to a different aromatic residue. An example is a mutation of Phe102 of cAMP to Trp146 of Rho kinase. In this case, two possibilities existed for matching the asymmetric indole ring to the symmetric phenyl ring. Molecular mechanical energy calculations were carried out for each possibility to select the conformation.

(3) Mutation to proline was conducted by keeping the ϕ and ψ torsional angles. Fortunately in this study, all such mutations occurred for the amino acid residues whose backbone conformation were compatible with those allowed for proline;[24] Ala124 to Pro168 ($\phi = -60$, $\psi = -26$); His260 to Pro311 (-101, -5); Lys295 to Pro347 (-46, -44); Glu341 to Pro393 (-59, 138), and Cys343 to Pro395 (-133, 57).

(4) If mutation from Gly, Ala, or Pro to other amino acid residue or 'different/larger' type mutation occurred, the sequence alignment with CDK2 or IRK was referred. If one found an identical amino acid type, the side-chain structure was taken from either CDK2 or IRK. For example, Val123 of cAPK corresponds to Met167 of Rho kinase. In IRK, the corresponding amino acid residue is Met1079. The side chain of the methionyl residue was transplanted to the Rho kinase model. Similarly Leu49 of cAPK was mutated using the side-chain structure of the corresponding isoleucyl residue of CDK2 (Ile10) to model Ile93 of Rho kinase.

(5) Residues whose side-chain conformation could not be determined by the rule described above were modeled by a conformational search (tweak search algorithm available in SYBYL package).

After the modeling, energy minimization using SYBYL-MAXIMIN2 software employing the force field parameter and atomic charge of Kollman was carried out.[25] The backbone atoms except for the modeled loops were fixed during this minimization.

The ligand-binding site was defined by those residues that locate within 4 Å from a super-ligand molecule. The super-ligand molecule was created by superimposing ligand molecules, ATP, H7, and staurosporin taken from the complex crystal structures of CDK2 (1HCL), cAPK (1YDR), and cAPK (1STC), respectively. The ligand-binding site involved 27 amino acid residues. They were Ile93, Gly94, Arg95, Gly96, Ala97, Val101, Ala114, Lys116, Glu135, Met139, Val148, Met164, Glu165, Tyr166, Met167, Pro168, Gly170, Asp171, Asp209, Lys211, Asp213, Asn214, Leu216, Ala226, Asp227, Phe228, and Phe379.

12.8. Docking simulation

A ligand molecule was placed in the active site in such way that the hydrogen bond acceptor atom took the position of N2 of H7 and the aromatic plane was in the plane defined by the isoquinoline ring of H7. The initial conformation of the ligand was first given interactively so that the ligand would reside in the enzyme pocket. The atomic charge of the ligand molecule was the MOPAC charge. All single bonds of a ligand molecule were selected as rotatable bonds except those in the ring system. When a test ligand included a chiral center(s), each configurational isomer model was built and considered independently. Similarly, when a cyclic system such as the pyperidine ring was included in a test ligand, the conformational models of the ring system, that is boat and chair forms, were prepared and docked independently. The *cis/trans* isomers were modeled for ligands that include the urea moiety. Atoms in the ligand-binding site and atoms within 4 Å of the ligand-binding site were used to calculate the docking interaction energy (total of 988 atoms including hydrogen atoms). Side-chain bonds of the amino acid residues that orient toward the inside of the ligand-binding pocket, Val101, Lys116, Glu135, Val148, Asp213, Asn214, Leu216, Asp227, and Phe379 were selected as the rotatable bonds. The atomic charge for the protein is from the Kollman all-atom force filed parameter available in the SYBYL package.

12.9. Chemistry

Analytical data were recorded for the compounds described below using the following general procedures. Proton NMR spectra were recorded using a Lambda 400 (Nippon Densi Datum, JEOL); chemical shifts were recorded in ppm (σ) from an internal tetramethylsilane standard as 0 ppm or internal chloroform as 7.24 ppm in deuterochloroform. Coupling constants (J) were recorded in Hz. Mass spectra (MS) were recorded using the PLATFORM-LC (Micromass) spectrometer. Melting points were taken using an electrothermal melting point apparatus and are uncorrected. The reagents were purchased from commercial sources.

12.9.1. *N*-(4-Pyridyl)-*N'*-(2,4,6-trichlorophenyl)urea (4a).
To a solution of 4-aminopyridine (500 mg, 3.56 mmol) in toluene (5 mL) was added 2,4,6-trichlorophenylisocyanate (504 mg, 3.56 mmol) at rt. The reaction mixture was stirred at 80 °C for 3 h and diluted with ether. The resulting precipitate was collected by filtration, washed with ether, and dried up in vacuo to give the title compound as a colorless solid (819 mg, 2.60 mmol, 87% yield in this step). Mp 205 °C. ^{1}H NMR (CDCl$_3$, 400 MHz) δ 7.43 (dd, $J = 1.7$ Hz, 4.9 Hz, 2H), 7.62 (s, 2H), 8.35 (dd, $J = 1.7$ Hz, 4.9 Hz, 2H), 8.48 (s, 1H), 9.45 (s, 1H). MS (ESI) m/z 315 (M-1)$^-$. Anal. Calcd for C$_{12}$H$_8$ON$_3$Cl$_3$: C, 44.27; H, 2.79; N, 2.91. Found: C, 44.71; H, 2.63; N, 12.13.

12.9.2. *N*-(4-Pyridyl)-*N'*-(2,6-dichlorophenyl)urea (4b).

Compound **4b** was prepared from 2,6-dichlorophen-ylisocyanate in a manner similar to that described for **4a**, except washing the precipitate with *n*-hexane, with a yield of 88% as a colorless solid. Mp 168–170 °C. ^{1}H NMR (CDCl$_3$, 400 MHz) δ 7.20 (t, $J = 7.8$ Hz, 1H), 7.39 (d, $J = 8.3$ Hz, 2H), 7.49 (dd, $J = 1.7$ Hz, 4.9 Hz, 2H), 8.31 (dd, $J = 1.5$ Hz, 5.1 Hz, 2H). MS (ESI) m/z 281 (M$-$1)$^-$.

12.9.3. *N*-(4-Pyridyl)-*N'*-(2,4-dichlorophenyl)urea (4c).

Compound **4c** was prepared from 2,4-dichlorophen-ylisocyanate in a manner similar to that described for **4a**, except washing the precipitate with *n*-hexane, with a yield of 93% as a colorless solid. Mp 244 °C. ^{1}H NMR (CDCl$_3$, 400 MHz) δ 7.31 (dd, $J = 2.4$ Hz, 9.0 Hz, 1H), 7.48 (d, $J = 2.4$ Hz, 1H), 7.53 (dd, $J = 1.7$ Hz, 4.9 Hz, 2H), 8.17 (d, $J = 9.0$ Hz, 1H), 8.33 (dd, $J = 1.7$ Hz, 4.9 Hz, 2H). MS (ESI) m/z 281 (M$-$1)$^-$.

12.9.4. *N*-(4-Pyridyl)-*N'*-(2-chlorophenyl)urea (4d).

Compound **4d** was prepared from 2-chlorophenyliso-cyanate in a manner similar to that described for **4a** with a yield of 76% as a colorless solid. ^{1}H NMR (CDCl$_3$, 400 MHz) δ 6.98 (m, 2H), 7.29 (dd, $J = 8.2$ Hz, 1.5 Hz, 1H), 7.38 (d, $J = 6.2$ Hz, 2H), 8.09 (dd, $J = 8.2$ Hz, 1.5 Hz, 1H), 8.38 (d, $J = 6.2$ Hz, 2H). MS (ESI) m/z 246 (M$-$1)$^-$.

12.9.5. *N*-(4-Pyridyl)-*N'*-phenylurea (4e).

Compound **4e** was prepared from phenylisocyanate in a manner similar to that described for **4a**, except washing the precipitate with *n*-hexane, with a yield of 88% as a colorless solid. ^{1}H NMR (CDCl$_3$, 400 MHz) δ 7.2–7.3 (m, 5H), 7.33 (d, $J = 5.7$ Hz, 2H), 8.30 (d, $J = 5.7$ Hz, 2H). MS (ESI) m/z 212 (M$-$1)$^-$.

12.9.6. *N*-(4-Pyridyl)-*N'*-(2,6-fluorophenyl)urea (4f).

Compound **4f** was prepared from 2,6-difluorophenylis-ocyanate in a manner similar to that described for **4a**, except washing the precipitate with *n*-hexane, with a yield of 93% as a colorless solid. ^{1}H NMR (CDCl$_3$, 400 MHz) δ 6.95 (d, $J = 8.3$ Hz, 1H), 6.97 (d, $J = 8.1$ Hz, 1H), 7.19 (t, $J = 8.3$ Hz, 1H), 7.48 (dd, $J = 1.5$ Hz, 5.1 Hz, 2H), 8.31 (dd, $J = 1.5$ Hz, 4.9 Hz, 2H). MS (ESI) m/z 248 (M$-$1)$^-$.

12.9.7. *N*-(4-Pyridyl)-*N'*-[2-fluoro-6-(trifluoromethyl)-phenyl]urea (4g).

Compound **4g** was prepared from 2-fluoro-6-(trifluoromethyl)phenylisocyanate in a manner similar to that described for **4a**, except washing the precipitate with EtOAc, with a yield of 44% as a col-orless solid. Mp 231–232 °C. ^{1}H NMR (CDCl$_3$, 400 MHz) δ 7.45 (dd, $J = 1.6$ Hz, 4.8 Hz, 2H), 7.48–7.64 (m, 3H), 8.34 (s, 1H), 8.39 (dd, $J = 1.6$ Hz, 4.8 Hz, 2H), 9.28 (s, 1H). MS (ESI) m/z 298 (M$-$1)$^-$.

12.9.8. *N*-(2,6-Dichlorobenzyl)-*N'*-(4-pyridyl)urea (5a).

To a solution of 2,6-dichlorophnylacetic acid (150 mg, 0.78 mmol) in toluene (0.5 mL) was added triethylamine (0.13 mL, 0.93 mmol), diphenylphosphorylazide (0.2 mL, 0.93 mmol), stirred at 110 °C for 1 h, and allowed to cool to rt. 4-Aminopyridine (128 mg, 0.78 mmol in DMF) was added and temperature was raised to 110 °C for 2 h. Water and EtOAc were added to the reaction mixture. The precipitate was filtered and washed with EtOAc to give the title compound as a white solid (76 mg, 32% yield). Mp 216 °C. ^{1}H NMR (CDCl$_3$, 400 MHz) δ 6.08 (d, $J = 5.3$ Hz, 2H), 6.73 (t, $J = 5.4$ Hz, 1H), 7.34 (dd, $J = 1.6$ Hz, 4.9 Hz, 2H), 7.38 (dd, $J = 1.2$ Hz, 7.3 Hz, 1H), 7.51 (d, $J = 7.8$ Hz, 2H), 8.28 (dd, $J = 1.7$ Hz, 4.9 Hz, 2H), 8.84 (s, 1H). MS (ESI) m/z 295 (M$-$1)$^-$. Anal. Calcd for C$_{13}$H$_{11}$Cl$_2$N$_3$O: C, 52.72; H, 3.745; N, 14.19. Found: C, 52.65; H, 3.64; N, 13.98.

12.9.9. *N*-(2,4-Dichlorobenzyl)-*N'*-(4-pyridyl)urea (5b).

Compound **5b** was prepared from 2,4-dichlorophen-ylacetic acid in a manner similar to that described for **5a**, except purification by silica gel column chromatography (CHCl$_3$–MeOH), with a yield of 30% as a colorless solid. Mp 167–169 °C. ^{1}H NMR (CDCl$_3$, 400 MHz) δ 4.35 (d, $J = 5.9$ Hz, 2H), 6.94 (t, $J = 6.0$ Hz, 1H), 7.37 (dd, $J = 1.6$ Hz, 4.8 Hz, 2H), 7.39 (d, $J = 8.4$ Hz, 1H), 7.44 (dd, $J = 2.1$ Hz, 8.4 Hz, 1H), 7.61 (d, $J = 2.2$ Hz, 1H), 8.29 (dd, $J = 1.5$ Hz, 4.9 Hz, 2H), 9.17 (s, 1H). MS (ESI) m/z 295 (M$-$1)$^-$.

12.9.10. *N*-(2-Chlorobenzyl)-*N'*-(4-pyridyl)urea (5c).

Compound **5c** was prepared from 2-chlorophenylacetic acid in a manner similar to that described for **5a**, except purification by silica gel column chromatography (CHCl$_3$–MeOH), with a yield of 38% as a colorless solid. Mp 130–131 °C. ^{1}H NMR (CDCl$_3$, 400 MHz) δ 4.38 (d, $J = 6.1$ Hz, 2H), 6.90 (t, $J = 5.9$ Hz, 1H), 7.28–7.41 (m, 4H), 7.37 (dd, $J = 1.5$ Hz, 4.9 Hz, 2H), 7.45 (dd, $J = 1.5$ Hz, 7.7 Hz, 1H), 8.29 (dd, $J = 1.5$ Hz, 4.9 Hz, 2H), 9.13 (s, 1H). MS (ESI) m/z 260 (M$-$1)$^-$.

12.9.11. *N*-Benzyl-*N'*-(4-pyridyl)urea (5d).

To a solution of 4-aminopyridine (50 mg, 0.53 mmol) in toluene (1 mL) was added benzylisocyanate (71 mg, 0.53 mmol) and stirred at 110 °C for 2 h. Water and EtOAc were added to the reaction mixture. EtOAc layer was washed with water and saturated NaCl aq, dried over anhydrous Na$_2$SO$_4$, and solvent was removed. The residue was purified by silica gel column chromatography (CHCl$_3$–MeOH). The title compound was obtained as a colorless solid (18 mg, 15% yield). Mp 156–157 °C. ^{1}H NMR (CDCl$_3$, 400 MHz) δ 4.31 (d, $J = 5.9$ Hz, 2H), 6.85 (t, $J = 5.9$ Hz, 1H), 7.24 (tt, $J = 1.7$ Hz, 6.8 Hz, 1H), 7.28–7.36 (m, 4H), 7.37 (dd, $J = 1.6$ Hz, 4.8 Hz, 2H), 8.28 (d, $J = 6.1$ Hz, 2H), 9.01 (s, 1H). MS (ESI) m/z 226 (M$-$1)$^-$.

12.9.12. *N*-(2,6-Difluorobenzyl)-*N'*-(4-pyridyl)urea (5e). Compound **5e** was prepared from 2,6-difluorophenylacetic acid in a manner similar to that described for **5a**, except purification by silica gel column chromatography (CHCl$_3$–MeOH), with a yield of 57% as a colorless solid. Mp 153–155 °C. ^{1}H NMR (CDCl$_3$, 400 MHz) δ 4.39 (d, $J = 5.4$ Hz, 2H), 6.84 (t, $J = 5.7$ Hz, 1H), 7.10 (t, $J = 8.2$ Hz, 2H), 7.33 (dd, $J = 1.6$ Hz, 4.8 Hz, 2H), 7.40 (dt, $J = 1.6$ Hz, 8.3 Hz, 1H), 8.27 (dd, $J = 1.6$ Hz, 4.8 Hz, 2H), 8.87 (s, 1H). MS (ESI) m/z 262 (M−1)$^-$.

12.9.13. *N*-[2-Fluoro-6-(trifluoromethyl)benzyl]-*N'*-(4-pyridyl)urea (5f). Compound **5f** was prepared from 2-fluoro-6-trifluoromethylphenylacetic acid in a manner similar to that described for **5a**, except purification by silica gel column chromatography (CHCl$_3$–MeOH), with a yield of 55% as a colorless solid. Mp 138–139 °C. ^{1}H NMR (CDCl$_3$, 400 MHz) δ 4.51 (d, $J = 4.9$ Hz, 2H), 6.69 (t, $J = 5.0$ Hz, 1H), 7.34 (dd, $J = 1.5$ Hz, 4.9 Hz, 2H), 7.59–7.64 (m, 3H), 8.28 (s, 2H), 8.28 (d, $J = 6.3$ Hz, 2H), 8.82 (s, 1H). MS (ESI) m/z 310 (M−1)$^-$.

12.9.14. *N*1-(4-Pyridyl)-2-(2,6-dichloro-4-fluorophenoxy)-acetamide (6a). To a solution of 2,6-dichloro-4-fluorophenol (2.0 g, 11.05 mmol) in acetonitrile (10 mL), K$_2$CO$_3$ (1.83 g, 13.26 mmol), and methylbromoacetate (1.69 g, 11.05 mmol) was added and stirred at 80 °C for 1 h. Water was added to the reaction mixture and the mixture was extracted with EtOAc. The EtOAc layer was washed with water and saturated NaCl aq, dried over anhydrous Na$_2$SO$_4$, and the solvent was removed. The resulting 2,6-dichloro-4-fluorophenoxyacetic acid ethyl ester was obtained as a white powder (2.66 g, 95.2%).

To the solution of the ester (2.66 g, 10.51 mmol) in EtOH, 5% aqueous NaOH (20 mL) was added and stirred at 80 °C for 1 h. The reaction mixture was concentrated, acidified to pH 4 with 5% aqueous HCl, and extracted with EtOAc. The EtOAc layer was washed with water and saturated NaCl aq, dried over anhydrous Na$_2$SO$_4$, and dried in vacuo, to give 2,6-dichloro-4-fluorophenoxyacetic acid (2.31 g, 4.18 mmol, 92%) as a colorless solid.

To a solution of the acetic acid (2.31 g, 4.18 mmol) in DMF (4 mL) was added 4-aminopyridine (393 mg, 4.18 mmol), WSC–HCl (946 mg, 5.0 mmol) and HOBt–H$_2$O (678 mg, 5.0 mmol). The reaction mixture was stirred for 3.5 h at rt. To the reaction mixture, water was added and extracted with EtOAc. The organic layer was washed with water and saturated NaCl aq, dried over anhydrous Na$_2$SO$_4$, and concentrated in vacuo. The crude material was purified by silica gel column chromatography to afford the title compound (155 mg, 11.8%) as colorless solid. Mp 126 °C. ^{1}H NMR (CDCl$_3$, 400 MHz) δ 4.63 (s, 2H), 7.15 (d, $J = 7.8$ Hz, 2H), 7.59 (dd, $J = 1.6$ Hz, 4.8 Hz, 2H), 8.57 (dd, $J = 1.5$ Hz, 4.9 Hz, 2H); MS (ESI) m/z 314 (M−1)$^-$. Anal. Calcd for C$_{13}$H$_9$Cl$_2$FN$_2$O$_2$: C, 49.55; H, 2.88; N, 8.89. Found: C, 49.47; H, 2.98; N, 8.89.

12.9.15. *N*1-(4-Pyridyl)-2-(2,6-dichlorophenoxy)acetamide (6b). (1) 2,6-Dichloro-phenoxyacetic acid was prepared from 2,6-dichlorophenol in a manner similar to that described for 2,6-dichloro-4-fluorophenoxyacetic acid with a yield of 79% as a colorless solid.

(2) The compound **6b** was prepared from 4-aminopyridine in a manner similar to that described for the compound **6a** with a yield of 10% as a colorless solid. ^{1}H NMR (CDCl$_3$, 400 MHz) δ 3.74 (d, $J = 2.7$ Hz, 2H), 7.20–7.40 (m, 7H). MS m/z 297 (M+1)$^-$.

12.9.16. *N*-(2-Amino-4-pyridyl)-*N'*-(2,6-dichlorophenyl)-urea (7a). To a solution of 2,6-dichlorobenzoic acid (2.0 g, 10.5 mmol) in toluene (10 mL) was added triethylamine (1.89 mL, 12.6 mmol), diphenylphosphorylazide (2.7 mL, 12.6 mmol) and stirred at 110 °C for 1 h and allowed to cool to rt. 3,4-Diaminopyridine (1.14 g, 10.5 mmol in DMF) was added and temperature was raised to 110 °C for 2 h. The solid precipitated in the reaction mixture was filtered, washed with EtOAc, and dried up in vacuo to give the title compound as a colorless solid (440 mg, 14% yield). Mp 224–228 °C. ^{1}H NMR (DMSO, 400 MHz) δ 6.55 (br s, 2H), 6.78 (d, $J = 5.9$ Hz, 1H), 6.99 (t, $J = 7.6$ Hz, 1H), 7.30–7.35 (m, 1H), 7.53 (d, $J = 8.1$ Hz, 2H), 7.91 (d, $J = 6.1$ Hz, 1H), 8.30 (s, 1H), 8.62 (br s, 1H). MS (ESI) m/z 296 (M−1)$^-$.

12.9.17. *N*-(3,5-Dichloro-4-pyridyl)-*N'*-(2,6-dichlorophenyl)urea (7b). To a solution of 2,6-dichlorobenzoic acid (150 mg, 0.78 mmol) in toluene (0.5 mL) was added triethylamine (0.14 mL, 0.93 mmol), diphenylphosphorylazide (0.2 mL, 0.93 mmol) and stirred at 110 °C for 1 h and allowed to cool to rt. 4-Amino-3,5-dichloropyridine (128 mg, 0.78 mmol in DMF) was added and temperature was raised to 110 °C for 2 h. Water was added to the reaction mixture and the mixture was extracted with EtOAc. The EtOAc layer was washed with water and saturated NaCl aq, dried over anhydrous Na$_2$SO$_4$, and dried up in vacuo. The residue was washed with CHCl$_3$ and collected by filtration to give the title compound as a colorless solid (40 mg, 15% yield). Mp 250–255 °C. ^{1}H NMR (DMSO, 400 MHz) δ 7.28–7.36 (m, 1H), 7.52 (d, $J = 8.3$ Hz, 2H), 7.54 (d, $J = 7.6$ Hz, 2H), 8.44 (br s, 1H), 8.63 (s, 1H). MS (ESI) m/z 350 (M−1)$^-$.

12.9.18. *N*-(2,6-Dichloro-4-pyridyl)-*N'*-(2,6-dichlorophenyl)urea (7c). Compound **7c** was prepared from 4-amino-2,6-diaminopyridine in a manner similar to that described for **7a**, with a yield of 4% as a colorless solid. ^{1}H NMR (DMSO, 400 MHz) δ 7.38 (t, $J = 8.3$ Hz, 1H), 7.52 (d, $J = 8.3$ Hz, 2H), 7.55–7.58 (m, 3H), 8.43 (br s, 1H). MS (ESI) m/z 350 (M−1)$^-$.

12.9.19. *N*-(2-Chloro-4-pyridyl)-*N'*-(2,4,6-trichlorophenyl)urea (7d). Compound **7d** was prepared from 4-amino-2-chloropyridine and 2,4,6-trichlorophenylisocyanate, in a manner similar to that described for **4a** as a colorless solid. Mp 238 °C (dp). NMR (CD$_3$OD,

400 MHz) δ 7.29 (dd, J = 5.8 Hz, 1.9 Hz, 1H), 7.50 (s, 2H), 7.58 (d, J = 1.9 Hz, 1H), 8.06 (d, J = 5.8 Hz, 1H); MS (ESI) m/z 350 (M−1)⁻.

12.9.20. N-(2-Amino-4-pyridyl)-N′-(2,6-dichlorophenyl)-urea (7e). Compound **7e** was prepared from 2,4-diamino-pyridine and 2,6-dichlorophenylisocyanate, in a manner similar to that described for **4a** as a colorless solid. Mp 271–273 °C. NMR (CD₃OD, 400 MHz) δ 4.50 (s, 2H), 7.03 (t, J = 8.0 Hz, 1H), 7.29 (d, J = 8.0 Hz, 2H), 7.40 (m, 2H), 7.77 (m, 1H); MS (ESI) m/z 296 (M−1)⁻.

12.9.21. N-(2,6-Dichlorophenyl)-N,N′-dimethyl-N′-(4-pyridyl)urea (8). To a solution of N-(4-pyridyl)-N′-(2,6-dichlorophenyl)urea (**4b**) (50 mg, 0.18 mmol) in DMF (2 mL) was added sodium hydride (8.5 mg, 0.35 mmol) portionwise at rt. The reaction mixture was stirred at rt for 30 min and followed by addition of methyliodide (28 mg, 0.20 mmol). The resulting mixture was stirred at 110 °C for 1 h and quenched by addition of water. The aqueous layer was extracted with EtOAc. The combined organic layer was washed with saturated NaCl aq, dried over anhydrous Na₂SO₄, and concentrated in vacuo. The crude material was purified by silica gel column chromatography, eluting with CHCl₃–MeOH to afford the title compound (79 mg, 76.1%) as a colorless oil. ¹H NMR (CD₃OD, 400 MHz) δ 3.06 (s, 3H), 3.09 (s, 3H), 6.93 (d, J = 5.1 Hz, 2H), 7.01 (t, J = 8.3 Hz, 1H), 7.16 (d, J = 8.3 Hz, 2H), 8.11 (d, J = 5.1 Hz, 2H). MS (ESI) m/z 311 (M+1)⁺.

12.9.22. O-(4-Pyridylmethyl)-N-(2-chlorobenzyl)carbamate (9a). Compound **9a** was prepared from 2-chlorophenylacetic acid in a manner similar to that described for **9b** with a yield of 44% as a colorless solid. Mp 75 °C. ¹H NMR (CDCl₃–CD₃OD=25:1, 400 MHz) δ 4.49 (d, J = 6.4 Hz, 2H), 5.13 (s, 2H), 5.42 (br, 1H), 7.22–7.28 (m, 4H), 7.36–7.42 (m, 2H), 8.55–8.60 (m, 2H). MS (ESI) m/z 275 (M−1)⁻.

12.9.23. O-(4-Pyridylmethyl)-N-(2,6-dichlorophenyl)carbamate (9b). To a solution of 2,6-dichlorobenzoic acid (150 mg, 0.78 mmol) in toluene (1 mL) was added triethylamine (0.13 mL, 0.86 mmol), diphenylphosphorylazide (0.2 mL, 0.93 mmol) and stirred at 110 °C for 1 h and allowed to cool to rt. 4-Pyridylcarbinol (86 mg, 0.78 mmol) was added and temperature was raised to 110 °C for 2 h. Water was added to the reaction mixture and the mixture was extracted with EtOAc. The EtOAc layer was washed with water and saturated NaCl aq, dried over anhydrous Na₂SO₄, and dried up in vacuo. The residue was purified by a silica gel column chromatography (CHCl₃–MeOH) to give the title compound as a colorless solid (136 mg, 58% yield). Mp 114–116 °C. ¹H NMR (CDCl₃–CD₃OD=25:1, 400 MHz) δ 5.24 (s, 2H), 6.69 (br s, 1H), 7.20 (t, J = 8.2 Hz, 1H), 7.23–7.28 (m, 2H), 7.39 (d, J = 8.1 Hz, 2H), 8.60 (d, J = 5.9 Hz, 2H). MS (ESI) m/z 296 (M−1)⁻.

12.9.24. N-(2,6-Dichlorobenzyl)-N′-(3-amino-4-pyridyl)-urea (10). To a solution of 2,6-dichlorophenyl acetic acid (100 mg, 0.49 mmol) in toluene (0.5 mL) was added triethylamine (0.08 mL, 0.54 mmol) and diphenyl-phosphorylazide (162 mg, 0.63 mmol), stirred at 110 °C for 1 h, and allowed to cool to rt. 3,4-Diaminopyridine (53 mg, 0.49 mmol in DMF) was added and temperature was raised to 110 °C for 2 h. The crystal precipitated in the reaction mixture was filtered. The titled compound was obtained as colorless solid (35 mg, 23%). Mp 249–250 °C. ¹H NMR (DMSO, 400 MHz) δ 4.53 (d, J = 5.6 Hz, 2H), 5.85 (br s, 2H), 6.50 (t, J = 5.4 Hz, 1H), 6.60 (d, J = 5.6 Hz, 1H), 7.30–7.35 (m, 1H), 7.46 (d, J = 8.3 Hz, 2H), 7.64 (br s, 1H), 7.78 (d, J = 5.6 Hz, 1H), 8.11 (s, 1H). MS (ESI) m/z 310 (M−1)⁻.

12.9.25. N1-(2-Chloro-4-pyridyl)-2-(2,6-dichlorophen-oxy)acetamide (11). (1) 2,6-Dichloro-phenoxyacetic acid was prepared from 2,6-dichlorophenol in a manner similar to that described for 2,6-dichloro-4-fluorophen-oxyacetic acid with a yield of 79% as a colorless solid.

(2) The compound **11** was prepared from 4-amino-2-chloropyridine in a manner similar to that described for the compound **6a** with a yield of 10% as a dense oil. ¹H NMR (CD₃OD, 400 MHz) δ 7.03 (t, J = 8.0 Hz, 1H), 7.29 (d, J = 8.0, 2H), 7.40 (m, 2H), 7.77 (m, 1H).

12.9.26. N1-(1H-5-Indazolyl)-1-cyclohexanecarboxy-amide (12a). To a solution of cyclohexanecarboxylic acid (96 mg, 0.75 mmol) in DMF (1 mL) was added 5-amino-1H-indazole (100 mg, 0.75 mmol), WSC–HCl (173 mg, 0.9 mmol) and HOBt–H₂O (122 mg, 0.75 mmol). The reaction mixture was stirred for 16 h at rt. Water was added to the reaction mixture and extracted with EtOAc. The EtOAc layer was washed with water and saturated NaCl aq, dried over anhydrous Na₂SO₄, filtered, and concentrated. The title compound was obtained (80 mg, 44% yield) by silica gel column chromatography (CHCl₃–MeOH 95:5) Mp 230 °C (dp). ¹H NMR (CDCl₃, 400 MHz) δ 1.14–1.34 (m, 3H), 1.44 (q, J = 11.4 Hz, 2H), 1.62–1.69 (m, 1H), 1.73–1.84 (m, 4H), 2.33 (tt, J = 3.4 Hz, 11.6 Hz, 1H), 7.42 (dd, J = 1.5 Hz, 9.0 Hz, 1H), 7.45 (d, J = 9.0 Hz, 1H), 7.98 (s, 1H), 8.12 (s, 1H), 9.76 (s, 1H), 12.92 (s, 1H). MS (ESI) m/z 242 (M−1)⁻.

12.9.27. N1-(1H-5-Indazolyl)-1-cyclohexylacetamide (12b). Compound **12b** was prepared from cyclohexane acetic acid in a manner similar to that described for **12a** with a yield of 36% as a yellow solid. Mp 227–228 °C. ¹H NMR (CDCl₃, 400 MHz) δ 0.92–1.04 (m, 2H), 1.10–1.30 (m, 3H), 1.58–1.82 (m, 6H), 2.19 (d, J = 7.1 Hz, 2H), 7.39 (dd, J = 1.7 Hz, 9.0 Hz, 1H), 7.45 (d, J = 8.8 Hz, 1H), 7.98 (s, 1H), 8.11 (s, 1H), 9.81 (s, 1H), 12.92 (s, 1H,). MS (ESI) m/z 256 (M−1)⁻.

12.9.28. N1-(1H-5-Indazolyl)-2-(2,6-dichloro-4-fluoro-phenoxy)acetamide (12c). To a mixture of 2,6-dichloro-

4-fluorophenol (1.39 g, 7.69 mmol) and K_2CO_3 (1.40 g, 9.22 mmol) in acetonitrile (10 mL) was added methyl 2-bromoacetate (1.18 g, 7.69 mmol) dropwise at rt. The reaction mixture was stirred at 80 °C for 1 h, and evaporated for removal of acetonitrile. Water was added to the reaction mixture, and the aqueous layer was extracted with EtOAc. The EtOAc layer was washed with water, dried over anhydrous Na_2SO_4, and concentrated in vacuo. The residue was dissolved in EtOH (10 mL) followed by addition of 10% NaOH aq (5 mL). The mixture was stirred at 80 °C for 1 h and evaporated. The resulting mixture was acidified by 5% HCl aq. The aqueous layer was extracted with EtOAc. The combined organic layer was dried over anhydrous Na_2SO_4 and filtered. The filtrate was concentrated in vacuo to give 2,6-dichloro-4-fluorophenoxyacetic acid (1.79 g, 7.48 mmol). To a mixture of 2,6-dichloro-4-fluorophenoxyacetic acid (197 mg, 0.83 mmol), 5-amino-1*H*-indazole (100 mg, 0.75 mmol), HOBt–H_2O (122 mg, 0.90 mmol), and dimethylaminopyridine (5 mg) in DMF (3 mL) was added WSC–HCl (178 mg, 0.90 mmol) dropwise at 0 °C. The reaction mixture was stirred at rt for 18 h and quenched by addition of saturated $NaHCO_3$ aq. The aqueous layer was extracted with EtOAc three times. The combined organic layer was dried over anhydrous Na_2SO_4 and filtered. The filtrate was concentrated in vacuo. The residual oil was subjected to flash chromatography on silica gel, eluting with $CHCl_3$–MeOH (95:5), to give the title compound (210 mg, 0.59 mmol, 79% yield) as a colorless solid. [^1]H NMR (CDCl_3, 400 MHz) δ 4.62 (s, 2H), 7.49 (t, $J = 8.8$ Hz, 1H), 7.53 (dd, $J = 1.7$ Hz, 8.8 Hz, 1H), 7.59 (s, 1H), 7.61 (s, 1H), 8.03 (s, 1H), 8.16 (s, 1H), 10.06 (s, 1H), 12.99 (s, 1H). MS (ESI) m/z 353 (M−1)$^-$.

12.9.29. *N*1-(1*H*-6-Indazolyl)-1-cyclohexanecarboxy-amide (13a).
Compound 13a was prepared from 6-amino-1*H*-indazole in a manner similar to that described for 12a with a yield of 10% as a colorless solid. Mp 230 °C (dp). ^{1}H NMR (CDCl_3, 400 MHz) δ 1.10–1.82 (m, 11H), 7.07 (d, $J = 8.8$ Hz, 1H), 7.62 (d, $J = 8.5$ Hz, 1H), 7.93 (s, 1H), 8.11 (s, 1H), 9.94 (s, 1H), 12.87 (br, 1H). MS (ESI) m/z 242 (M−1)$^-$.

12.9.30. *N*1-(1*H*-6-Indazolyl)-1-cyclohexylacetamide (13b).
Compound 13b was prepared from 6-amino-1*H*-indazole and cyclohexaneacetic acid in a manner similar to that described for 12a with a yield of 30% as a yellow solid. Mp 192–193 °C. ^{1}H NMR (CDCl_3, 400 MHz) δ 0.94–1.85 (m, 11H), 2.23 (d, $J = 7.1$ Hz, 2H), 7.09 (dd, $J = 1.7$ Hz, 8.5 Hz, 1H), 7.66 (d, $J = 8.5$ Hz, 1H), 7.97 (s, 1H), 8.16 (s, 1H), 10.03 (br, 1H), 12.91 (br, 1H). MS (ESI) m/z 256 (M−1)$^-$.

12.9.31. *N*1-(1*H*-6-Indazolyl)-2-(2,6-dichloro-4-fluoro-phenoxy)acetamide (13c).
Compound 13c was prepared from 6-amino-1*H*-indazole in a manner similar to that described for 12c as a yellow solid. Mp 219–221 °C. ^{1}H NMR (DMSO-d_6, 400 MHz) δ 5.43 (s, 2H), 6.69 (d, $J = 8.5$ Hz, 1H), 7.46 (s, 1H), 7.47 (d, $J = 8.5$ Hz, 1H),

7.59 (s, 1H), 7.63 (s, 1H), 8.12 (s, 1H); (ESI) m/z 353 (M−1)$^-$.

12.9.32. *N*-(1*H*-5-Indazolyl)-*N'*-(2,6-dichlorophenyl)urea (14a).
5-Amino-1*H*-indazole (100 mg, 0.75 mmol) and 2,6-dichlorophenylisocyanate (155 mg, 0,83 mmol) was dissolved in toluene and stirred at 110 °C for 4 h. Solvent was removed and the resulting residue was washed with *n*-hexane to give the title compound (232 mg, 97% yield) as a colorless solid. Mp 275 °C (dp). ^{1}H NMR (CDCl_3, 400 MHz) δ 7.29 (d, $J = 8.8$ Hz, 1H), 7.33 (dd, $J = 1.7$ Hz, 8.8 Hz, 1H), 7.45 (d, $J = 8.8$ Hz, 1H), 7.52 (d, $J = 8.8$ Hz, 1H), 7.89 (dd, $J = 1.7$ Hz, 8.8 Hz, 1H), 7.96 (s, 1H), 8.14 (s, 1H), 8.86 (s, 1H). MS (ESI) m/z 320 (M−1)$^-$.

12.9.33. *N*-(1*H*-5-Indazolyl)-*N'*-(benzyl)urea (14b).
To a solution of 5-amino-1*H*-indazole (66 mg, 0.50 mmol) dissolved in toluene (1 mL) and trace amount of DMF, benzylisocyanate (0.061 mL, 0.5 mmol) was added and stirred at 110 °C for 3 h. Water was added to the reaction mixture and extracted with EtOAc. The EtOAc layer was washed with water and saturated NaCl aq, dried over anhydrous Na_2SO_4, filtered, and concentrated. The crude material was purified by silica gel column chromatography ($CHCl_3$–MeOH 95:5) to give the title compound (21 mg, 16% yield) as a colorless solid. ^{1}H NMR (CDCl_3, 400 MHz) δ 4.31 (d, $J = 5.9$ Hz, 2H), 6.53 (t, $J = 5.9$ Hz, 1H), 7.21–7.28 (m, 2H), 7.29–7.36 (m, 4H), 7.41 (d, $J = 8.8$ Hz, 1H), 7.85 (s, 1H), 7.93 (s, 1H,), 8.46 (s, 1H), 12.84 (s, 1H). MS (ESI) m/z 265 (M−1)$^-$.

12.9.34. *N*-(1*H*-6-Indazolyl)-*N'*-(2,6-dichlorophenyl)urea (15).
Compound 15 was prepared from 6-amino-1*H*-indazole in a manner similar to that described for 14a as a yellow solid. Mp 264–267 °C. NMR (CD_3OD, 400 MHz) δ 6.91 (dd, $J = 7.9$ Hz, 1.8Hz, 1H), 7.19 (t, $J = 8.0$ Hz, 1H), 7.39 (d, $J = 8.0$ Hz, 2H), 7.58 (dd, $J = 7.9$ Hz, 0.8 Hz, 1H), 7.84 (m, 1H), 7.85 (s, 1H); MS (ESI) m/z 320 (M−1)$^-$.

12.9.35. *N*-(1*H*-5-Indazolyl)-*N*-(4-piperizyl)amine (16a).
To a suspension of 4-hydroxypiperizine (1.01 g, 10 mmol) in 3 M NaOH aq (10 mL) was added a solution of di-*tert*-butyl dicarbonate (2.40 g, 11 mmol) in THF (10 mL) dropwise at 0 °C. The reaction mixture was stirred at rt for 1 h and evaporated for removal of THF. The aqueous layer was extracted with EtOAc. The organic layer was dried over anhydrous Na_2SO_4 and filtered. The filtrate was concentrated in vacuo to give 4-(*tert*-butyloxycarbonyl)piperizinone. To the piperizinone, triethylamine (2 mL) in anhydrous DMSO (10 mL) was added followed by addition of sulfur trioxide–trimethylamine complex (4.44 g, 20 mmol) portionwise at 0 °C. The reaction mixture was stirred at rt for 18 h and quenched by addition of saturated $NaHCO_3$ aq. The aqueous layer was extracted with EtOAc. The EtOAc layer was dried over anhydrous

Na$_2$SO$_4$ and filtered. The filtrate was concentrated in vacuo. To the residue, 5-amino-1H-indazole (0.98 g, 7.4 mmol) dissolved in MeOH (10 mL) and AcOH (0. 2 mL) were added. To the solution, BH$_3$–pyridine complex (1.0 mL, 10 mmol) was added dropwise at 0 °C. The reaction mixture was stirred at rt for 18 h and quenched by addition of saturated NaHCO$_3$ aq. The aqueous layer was extracted with CHCl$_3$. The CHCl$_3$ layer was dried over anhydrous Na$_2$SO$_4$ and filtered. The filtrate was concentrated in vacuo. The residual oil was subjected to flash chromatography on silica gel, eluting with CHCl$_3$–MeOH (95:5), to give *tert*-butyl 4-(1H-5-indazol-ylamino)-1-piperizinecarboxylate as yellow dense oil (2.30 g, 7.20 mmol, 72% yield in three steps).

To a solution of *tert*-butyl-4-(1H-5-indazolylamino)-1-piperizinecarboxylate (450 mg, 1.42 mmol) in CHCl$_3$ (3 mL) was added 95% trifluoroacetic acid (3 mL) dropwise at rt. The reaction mixture was stirred at rt for 3 h and concentrated in vacuo to give the title compound as a colorless solid having mp of 172–176 °C (420 mg, 1.32 mmol, 93% yield in this step). ^{1}H NMR (CDCl$_3$, 400 MHz) δ 1.29 (m, 2H), 1.95 (m, 2H), 2.59 (m, 2H), 2.98 (m, 2H), 3.22 (m, 1H), 6.82 (s, 1H), 6.86 (d, $J = 8.8$ Hz, 1H), 7.24 (d, $J = 8.8$ Hz, 2H), 7.73 (s, 1H); MS (ESI) m/z 217 (M+1)$^+$.

12.9.36. *N*-(1-Ethyl-4-piperidyl)-*N*-(1H-5-indazolyl)-amine (16b).

Compound **16b** was prepared from 1-ethyl-4-piperidone in a manner similar to that described for **16c** with a yield of 41% as a yellow dense oil. ^{1}H NMR (CDCl$_3$, 400 MHz) δ 1.06 (t, $J = 7.3$ Hz, 3H), 1.42–1.53 (m, 2H), 2.02–2.17 (m, 4H), 2.42 (q, $J = 7.1$ Hz, 2H), 2.86–2.95 (m, 2H), 3.21–3.33 (m, 1H), 6.70–6.76 (m, 2H), 7.23 (d, $J = 8.5$ Hz, 1H), 7.81 (s, 1H). MS (ESI) m/z 245 (M+1)$^+$.

12.9.37. *N*-(1-Benzyl-4-piperidyl)-*N*-(1H-5-indazolyl)-amine (16c).

To a solution of 1-benzylpiperidone (635 mg, 3.4 mmol), 5-amino-1H-indazole (532 mg, 4 mmol), and AcOH (0.20 mL) in MeOH (10 mL) was added BH$_3$–pyridine complex (0.51 mL, 5 mmol) dropwise at 0 °C. The reaction mixture was stirred at rt for 18 h and quenched by addition of saturated NaHCO$_3$ aq. The aqueous layer was extracted with CHCl$_3$. The CHCl$_3$ layer was dried over anhydrous Na$_2$SO$_4$ and filtered. The filtrate was concentrated in vacuo. The residual oil was subjected to flash chromatography on silica gel, eluting with CHCl$_3$–MeOH (95:5), to give the title compound as a yellow solid (1.00 g, 3.26 mmol, 82% yield). Mp 166 °C. ^{1}H NMR (CDCl$_3$, 400 MHz) δ 1.46–1.59 (m, 2H), 2.05–2.12 (m, 2H), 2.15–2.25 (m, 2H), 2.85–2.93 (m, 2H), 3.27–3.37 (m, 1H), 3.56 (s, 2H), 6.77–6.82 (m, 2H), 7.24–7.35 (m, 6H), 7.88 (s, 1H). MS (ESI) m/z 307 (M+1)$^+$.

12.9.38. *N*-(1-Ethyl-4-piperidyl)-*N*-(1H-6-indazolyl)-amine (17).

Purchased from ChemBridge.

12.9.39. *N*-(1-Benzyl-4-piperidyl)-*N*-(1H-5-indolyl)amine (18).

Compound **18** was prepared from 5-amino-1H-indole in a manner similar to that described for **16c** with a yield of 73% as a yellow solid. ^{1}H NMR (CDCl$_3$, 400 MHz) δ 1.5–1.7 (m, 4H), 1.9–2.1 (m, 2H), 2.80 (m, 2H), 3.25 (m, 1H), 3.49 (br s, 2H), 6.31 (m, 1H), 6.54 (dd, $J = 8.6$ Hz, 2.1 Hz, 1H), 6.78 (d, $J = 2.1$ Hz, 1H), 7.05 (dd, $J = 2.6$ Hz, 1H), 7.13 (d, $J = 8.6$ Hz, 1H), 7.2–7.3 (m, 5H), 7.84 (br s, 1H). MS (ESI) m/z 306 (M+1)$^+$.

12.9.40. *N*-(1-Benzyl-3-piperidyl)-*N*-(6-fluoro-1H-5-indazolyl)amine (19a).

(1) *5-Amino-6-fluoro-1H-indazole*. To a mixture of 5-fluoro-o-toluidine (6.25 g, 50 mmol) and potassium acetate (6.00 g, 60 mmol) in CHCl$_3$ (50 mL) was added acetic acid anhydride (15.0 g, 150 mmol) dropwise at 0 °C. The mixture was stirred at rt for 30 min, heated to 40 °C, and followed by addition of isoamyl nitrite (11.7 g, 100 mmol) dropwise at 40 °C. The reaction mixture was stirred at 60 °C for 18 h and quenched by addition of saturated NaHCO$_3$ aq. The aqueous layer was extracted with CHCl$_3$. The organic layer was dried over anhydrous Na$_2$SO$_4$ and filtered. The filtrate was concentrated in vacuo. The residual oil was subjected to chromatography on silica gel, eluting with CHCl$_3$–MeOH (9:1) to give 6-fluoro-1-acetyl-indazole.

A mixture of the residue in HCl–MeOH (200 mL) was stirred at 80 °C for 5 h and evaporated for removal of HCl–MeOH. The resulting residue was basified by saturated NaHCO$_3$ aq. The aqueous layer was extracted with EtOAc. The organic layer was dried over anhydrous Na$_2$SO$_4$ and filtered. The filtrate was concentrated in vacuo. The precipitate was washed with CHCl$_3$ to give 6-fluoro-1H-indazole as a brown solid (4.80 g, 35 mmol, 70% yield).

To a mixture of 6-fluoro-1H-indazole (4.80 g, 35 mmol) in 50% H$_2$SO$_4$ aq (20 mL) was added sodium nitrate (3.40 g, 40 mmol) portionwise at 0 °C. The resulting mixture was stirred at rt for 1 h, and quenched by addition of saturated NaHCO$_3$ aq. The aqueous layer was extracted with EtOAc. The organic layer was dried over anhydrous Na$_2$SO$_4$ and filtered. The filtrate was concentrated in vacuo. The residual solid was washed with CHCl$_3$ to give 5-nitro-6-fluoro-1H-indazole (3.00 g, 16 mmol).

To a mixture of 5-fluoro-5-nitro-1H-indazole (2.00 g, 11 mmol) in 50% HCl aq (10 mL) was added tin(II)chloride dihydrate (4.50 g, 20 mmol) portionwise at 0 °C. The resulting mixture was stirred at rt for 5 h, and quenched by addition of saturated NaHCO$_3$ aq. The aqueous layer was extracted with EtOAc. The organic layer was dried over anhydrous Na$_2$SO$_4$ and filtered. The filtrate was concentrated in vacuo. The residual solid was washed with CHCl$_3$ to give 5-amino-6-fluoro-1H-indazole (1.67 g, 11 mmol).

(2) Compound **19a** was prepared from 5-amino-6-fluoro-1H-indazole in a manner similar to that described for **16c** with a yield of 52% as a yellow solid. Mp 137–

140 °C. ^{1}H NMR (CDCl$_3$, 400 MHz) δ 1.52–1.64 (m, 2H), 2.09 (br d, $J = 10.0$ Hz, 2H), 2.23 (br t, $J = 10.8$ Hz, 2H), 2.91 (br d, $J = 11.6$ Hz, 2H), 3.32 (br s, 1H), 3.58 (s, 2H), 6.83 (d, $J = 8.0$ Hz, 1H), 7.08 (d, $J = 13.6$ Hz, 1H), 7.23–7.27 (m, 1H), 7.28–7.35 (m, 4H), 7.88 (s, 1H). MS (ESI) m/z 325 (M+1)$^+$.

12.9.41. N-(1-Benzyl-4-piperidyl)-N-(6-methoxy-1H-5-indazolyl)amine (19b).

(1) *5-Amino-6-methoxy-1H-indazole*. The compound was prepared from 5-methoxy-2-methylaniline in a manner similar to that described for the compound, 5-amino-6-fluoro-1H-indazole, with a yield of 75% as a brown solid.

(2) Compound **19b** was prepared from 5-amino-6-methoxy-1H-indazole in a manner similar to that described for **16c** with a yield of 40% as a yellow solid. Mp 161–164 °C. ^{1}H NMR (CDCl$_3$, 400 MHz) δ 1.51–1.64 (m, 2H), 2.11 (br d, $J = 11.2$ Hz, 2H), 2.23 (br t, $J = 10.8$ Hz, 2H), 2.90 (br d, $J = 11.6$ Hz, 2H), 3.32 (br s, 1H), 3.57 (s, 2H), 3.86 (s, 3H), 6.71 (s, 1H), 6.75 (s, 1H), 7.23–7.29 (m, 1H), 7.30–7.40 (m, 4H), 7.81 (s, 1H). MS (ESI) m/z 337 (M+1)$^+$.

12.9.42. N1-(1-Benzyl-4-piperidyl)-N1-(1H-5-indazolyl)acetamide (19c).

To a mixture of N-(1-benzyl-4-piperidyl)-N-(1H-5-indazolyl)amine (307 mg, 1.0 mmol) and pyridine (220 mg, 2.4 mmol) in CHCl$_3$ (1 mL) was added acetylchloride (170 mg, 2.4 mmol) dropwise at rt. The reaction mixture was stirred at rt for 18 h, and quenched by addition of saturated NaHCO$_3$ aq. The aqueous layer was extracted with CHCl$_3$. The CHCl$_3$ layer was dried over anhydrous Na$_2$SO$_4$ and filtered. The filtrate was concentrated in vacuo. The residual was dissolved in MeOH (1 mL) and HCl–MeOH (1 mL) was added. The reaction mixture was stirred at rt for 5 h and basified by addition of saturated NaHCO$_3$ aq. The aqueous layer was extracted with EtOAc. The organic layer was dried over anhydrous Na$_2$SO$_4$ and filtered. The filtrate was concentrated in vacuo. The residual oil was subjected to flash chromatography on silica gel, eluting with CHCl$_3$, to give the title compound as yellow dense oil (321 mg, 0.95 mmol, 95% yield). ^{1}H NMR (CDCl$_3$, 400 MHz) δ 1.23–1.40 (m, 1H), 1.50–1.70 (m, 1H), 1.70–1.80 (m, 1H), 1.82–1.92 (m, 1H), 2.02 (s, 3H), 2.11–2.28 (m, 2H), 2.91–3.08 (m, 2H), 3.48 (d, $J = 12.7$ Hz, 1H), 3.55 (d, $J = 13.0$ Hz, 1H), 4.66–4.76 (m, 1H), 6.92–6.98 (m, 1H), 7.20–7.27 (m, 6H), 7.52 (s, 1H), 8.05 (s, 1H). MS (ESI) m/z 349 (M+1)$^+$.

12.9.43. N1-(1-Benzyl-4-piperidyl)-N1-(1H-5-indazolyl)ethylamine (19d).

To a mixture of N1-(1-benzyl-4-piperidyl)-N1-(1H-5-indazolyl)acetamide (**19c**) (70 mg, 0.2 mmol) in THF (1 mL) was added 1M BH$_3$/THF (0.06 mL, 0.6 mmol) dropwise at rt. The reaction mixture was stirred at 60 °C for 3 h, and quenched by addition of 1 N HCl aq at 0 °C. The resulting mixture was stirred at 60 °C for 1 h and cooled to rt. The aqueous layer was extracted with CHCl$_3$. The CHCl$_3$ layer

was dried over anhydrous Na$_2$SO$_4$ and filtered. The filtrate was concentrated in vacuo. The residual oil was subjected to chromatography on silica gel, eluting with CHCl$_3$, to give the title compound as yellow dense oil (50 mg, 0.15 mmol, 75% yield). ^{1}H NMR (CDCl$_3$, 400 MHz) δ 0.99 (br s, 3H), 1.3–2.2 (m, 8H), 3.05 (m, 2H), 3.20 (br s, 2H), 3.30 (m, 1H), 7.03 (s, 1H), 7.05 (s, 1H), 7.2–7.3 (m, 6H), 7.87 (s, 1H). MS (ESI) m/z 335 (M+1)$^+$.

12.9.44. N-(1-Benzyl-4-piperidyl)-N-(3-methyl-1H-5-indazolyl)amine (19e).

(1) *5-Amino-3-methyl-1H-indazole*. To a mixture of 2-aminoacetophenone (1.35 g, 10 mmol) in 50% H$_2$SO$_4$ aq (20 mL) was added sodium nitrite (0.82 g, 12 mmol) portionwise at 0 °C. The resulting mixture was stirred at rt for 1 h, and followed by addition of tin(II)chloride dehydrate (6.76 g, 30 mmol). The reaction mixture was stirred at 0 °C for 1 h and diluted by water. The white solid was collected by filtration, and dried up in vacuo to give 3-methyl-1H-indazole (1.20 g, 9 mmol). The introduction of the amino group at the 5-position was performed in a manner similar to that described for the compound, 5-amino-6-fluoro-1H-indazole, with a yield of 88% as brown solid.

(2) Compound **19e** was prepared from 5-amino-3-methyl-1H-indazole in a manner similar to that described for **16c** with a yield of 55% as yellow dense oil. ^{1}H NMR (CDCl$_3$, 400 MHz) δ 1.50–1.75 (m, 2H), 2.00–2.11 (m, 2H), 2.15–2.40 (m, 2H), 2.56 (s, 3H), 2.89–3.00 (m, 2H), 3.25–3.37 (m, 1H), 3.57–3.67 (m, 2H), 6.51 (t, $J = 1.9$ Hz, 1H), 6.81 (dd, $J = 1.9$ Hz, 9.2 Hz, 1H), 7.23–7.32 (m, 5H), 7.47 (d, $J = 9.0$ Hz, 1H). MS (ESI) m/z 321 (M+1)$^+$.

12.9.45. N-(1-Benzyl-4-piperidyl)-N-(1-methyl-5-indazolyl)amine (19f).

Compound **19f** was prepared from N-(1-benzyl-4-piperidyl)-N-(1-H-5-indazolyl)amine (**16c**) in a manner similar to that described for **21b** as yellow dense oil. ^{1}H NMR (CDCl$_3$, 400 MHz) δ 1.5–1.8 (m, 4H), 2.0–2.2 (m, 2H), 2.8–2.9 (m, 2H), 3.2–3.3 (m, 1H), 3.5–3.6 (br s, 2H), 3.98 (s, 3H), 6.76 (m, 1H), 6.78 (dd, $J = 8.6$ Hz, 2.2 Hz, 1H), 7.18 (d, $J = 8.6$ Hz, 1H), 7.2–7.3 (m, 5H), 7.75 (s, 1H). MS (ESI) m/z 321 (M+1)$^+$.

12.9.46. N-(1-Propyl-3-piperidyl)-N-(1H-5-indazolyl)amine (20a).

3-Hydroxypiperidine (1.0 g, 9.8 mmol), K$_2$CO$_3$ (2.76 g, 41 mmol), and 1-bromopropane (1.23 g, 10 mmol) were stirred in acetonitrile (10 mL) for 12 h at rt, and quenched by water. The aqueous layer was extracted with EtOAc. The EtOAc layer was washed with saturated NaCl aq, dried over Na$_2$SO$_4$, filtered, and concentrated in vacuo to give N-propyl-3-hydroxypyperidine (1.10 g, 41 mmol). To a mixture of the crude N-propyl-3-hydorxypyperidine and triethyl amine (1.45 g, 15 mmol) in anhydrous DMSO (15 mL) was added sulfur trioxide trimethylamine complex (2.13 g, 15 mmol) and the reaction mixture was stirred for 12 h. Water was added to the reaction mixture and extracted with EtOAc. The EtOAc layer was washed with saturated

NaCl aq, dried over anhydrous Na_2SO_4, and concentrated in vacuo. The crude mixture was purified by silica gel column chromatography (hexane–EtOAc 1:1) to give *N*-propyl-3-piperidone (213 mg, 1.5 mmol). A mixture of the *N*-propyl-3-piperidone and 5-aminoindazole (200 mg, 1.5 mmol) in Ti(O-*i*-Pr)$_4$ (3 mL) was stirred for 1 h and followed by addition of MeOH (3 mL) and sodium borohydride (100 mg, 2.8 mmol). The reaction mixture was quenched by addition of water at 0 °C. The reaction mixture was extracted with CHCl$_3$. The CHCl$_3$ layer was washed with saturated NaCl aq, dried over anhydrous Na_2SO_4, and concentrated in vacuo. The residue was purified by silica gel column chromatography (CHCl$_3$–MeOH 9:1) to give the title compound (100 mg, 3.8%, total yield) as pale-yellow dense oil. ^{1}H NMR (CDCl$_3$, 400 MHz) δ 0.90 (t, $J = 7.4$ Hz, 3H), 1.59 (m, 4H), 2.11 (t, $J = 12.0$ Hz, 2H), 2.18 (t, $J = 10.0$ Hz, 2H), 2.38 (dd, $J = 9.8$ Hz, 2H), 2.97 (br d, $J = 11.4$ Hz, 2H), 3.33 (tt, $J = 9.8$ Hz, 11.4 Hz, 1H), 6.76 (d, $J = 9.0$ Hz, 1H), 6.81 (d, $J = 1.3$ Hz, 1H), 7.25 (d, $J = 9.0$ Hz, 1H), 7.88 (d, $J = 1.3$ Hz, 1H). MS (ESI) *m/z* 259 (M+1)$^+$.

12.9.47. *N*-(1-Benzyl-3-piperidyl)-*N*-(1*H*-5-indazolyl)-amine (20b). Compound **20b** was prepared from 1-benzyl-3-piperidone in a manner similar to that described for **16c** with a yield of 78% as yellow dense oil. ^{1}H NMR (CDCl$_3$, 400 MHz) δ 1.40–1.60 (m, 3H), 1.70–1.80 (m, 2H), 2.10–2.50 (m, 3H), 3.45 (s, 2H), 3.16–3.22 (m, 1H), 6.75 (dd, $J = 2.4$ Hz, 11.2 Hz, 2H), 7.15–7.28 (m, 6H), 7.78 (d, $J = 0.7$ Hz, 1H). MS (ESI) *m/z* 305 (M−1)$^-$.

12.9.48. *N*-(1*H*-5-Indazolyl)-*N*-tetrahydro-1*H*-3-pyrrorylamine (20c). Compound **20c** was prepared from 3-pyrrolidinol in a manner similar to that described for **16a** with a yield of 45% as yellow dense oil. ^{1}H NMR (CDCl$_3$, 400 MHz) δ 1.6–1.9 (m, 2H), 2.53 (m, 1H), 2.64 (m, 1H), 2.82 (m, 1H), 3.26 (m, 1H), 3.39 (m, 1H), 6.75 (d, $J = 6.8$ Hz, 1H), 6.78 (s, 1H), 7.26 (d, $J = 6.8$ Hz, 1H), 7.80 (s, 1H); (ESI) *m/z* 203 (M+1)$^+$.

12.9.49. *N*-(1-Benzyltetrahydro-1*H*-pyrrolyl)-*N*-(1*H*-5-indazolyl)amine (20d). Compound **20d** was prepared from 1-benzyl-3-pyrrolidone in a manner similar to that described for **16c** with a yield of 35% as yellow dense oil. ^{1}H NMR (CDCl$_3$, 400 MHz) δ 1.66–1.78 (m, 1H), 2.30–2.41 (m, 1H), 2.44–2.53 (m, 1H), 2.61–2.38 (m, 1H), 2.77–2.87 (m, 2H), 3.66 (s, 2H), 4.00–4.08 (m, 1H), 6.73–6.76 (m, 1H), 6.77–6.83 (m, 1H), 7.14–7.28 (m, 6H), 7.88 (s, 1H). MS (ESI) *m/z* 293 (M+1)$^+$.

12.9.50. *N*-(1-Benzyl-3-piperidyl)-*N*-(3-methyl-1*H*-5-indazolyl)amine (21a). Compound **21a** was prepared from 5-amino-3-methyl-1*H*-indazole and 1-benzyl-3-piperidone in a manner similar to that described for **16c** with a yield of 55% as yellow dense oil. ^{1}H NMR (CDCl$_3$, 400 MHz) δ 1.44–1.61 (m, 3H), 1.65–1.80 (m, 2H), 2.20–2.30 (m, 1H), 2.43 (s, 3H), 2.72–2.81 (m, 2H), 3.48 (d, $J = 4.1$ Hz, 2H), 3.53–3.60 (m, 1H), 6.65 (d,

$J = 2.0$ Hz, 1H), 673 (dd, $J = 2.2$ Hz, 8.8 Hz, 1H), 7.14 (d, $J = 8.8$ Hz, 1H), 7.22–7.30 (m, 5H). MS (ESI) *m/z* 321 (M+1)$^+$.

12.9.51. *N*-(1-Benzyl-3-piperidyl)-*N*-(1-methyl-5-indazolyl)amine (21b). A mixture of *N*-(1-benzyl-3-piperidyl)-*N*-(1*H*-5-indazolyl)amine (**20b**) (100 mg, 0.33 mmol), K$_2$CO$_3$ (50 mg, 0.36 mmol), and methyliodide (0.02 mL, 0.33 mmol) in DMF (2 mL) was stirred at 110 °C for 1 h. The resulting mixture was diluted with water. The aqueous layer was extracted with EtOAc. The organic layer was dried over anhydrous Na_2SO_4 and filtered. The filtrate was concentrated in vacuo. The residual oil was subjected to chromatography on silica gel, eluting with CHCl$_3$, to give the title compound as yellow dense oil (79 mg, 0.25 mmol, 76% yield). ^{1}H NMR (CDCl$_3$, 400 MHz) δ 1.4–1.6 (m, 4H), 1.6–1.8 (m, 2H), 2.3–2.4 (m, 2H), 3.4–3.6 (m, 3H), 3.93 (s, 3H), 6.71 (m, 1H), 6.77 (m, 1H), 7.13 (d, $J = 8.6$ Hz, 1H), 7.2–7.3 (m, 5H), 7.68 (s, 1H). MS (ESI) *m/z* 321 (M+1)$^+$.

12.9.52. *N*-(1-Benzyl-4-piperidyl)-*N*-(5-isoquinolyl)amine (22a). To a solution of 1-benzylpiperidone (150 mg, 0.79 mmol), 5-aminoisoquinoline (114 mg, 0.79 mmol), and AcOH (1 drop) in MeOH (5 mL) was added BH$_3$–pyridine complex (0.10 mL, 1 mmol) dropwise at 0 °C. The reaction mixture was stirred at rt for 18 h and quenched by addition of saturated NaHCO$_3$ aq. The aqueous layer was extracted with CHCl$_3$. The CHCl$_3$ layer was dried over anhydrous Na_2SO_4 and filtered. The filtrate was concentrated in vacuo. The residual oil was subjected to flash chromatography on silica gel, eluting with CHCl$_3$–MeOH (95:5), to give the title compound (47 mg, 0.15 mmol, 20% yield) as yellow dense oil. ^{1}H NMR (CDCl$_3$, 400 MHz) δ 1.5–1.7 (m, 4H), 2.1–2.2 (m, 2H), 2.2–2.3 (m, 2H), 3.59 (s, m, 3H), 6.77 (d, $J = 7.8$ Hz, 1H), 7.30 (d, $J = 7.8$ Hz, 1H), 7.2–7.4 (m, 5H), 7.43 (dd, $J = 7.8$ Hz, 1H), 7.52 (d, $J = 6.0$ Hz, 1H), 8.46 (d, $J = 6.0$ Hz, 1H), 9.14 (s, 1H). MS (ESI) *m/z* 318 (M+1)$^+$.

12.9.53. *N*-(5-Isoquinolyl)-*N*-(1-propyl-4-piperidyl)amine (22b). To a mixture of 4-piperidone monohydrate (300 mg, 2.6 mmol) and K$_2$CO$_3$ (540 mg, 3.9 mmol) in acetonitrile (5 mL) was added a solution of *n*-propylbromide (359 mg, 2.7 mmol) in acetonitrile (2 mL) dropwise at 0 °C. The reaction mixture was stirred at rt for 18 h and diluted with EtOAc. The mixture was filtered through Celite. The filtrate was concentrated in vacuo. A mixture of the residue and 5-aminoisoquinoline (208 mg, 1.4 mmol) was dissolved in titanium tetraisopropoxide (5 mL), and the reaction mixture was stirred at rt for 30 min. The mixture was diluted with MeOH (5 mL) and sodium borohydride (101 mg, 2.6 mmol) was added at 0 °C. The mixture was stirred at rt for 3 h, filtered through Celite, and quenched by addition of saturated NaHCO$_3$ aq. The mixture was extracted with EtOAc. The organic layer was dried over anhydrous Na_2SO_4 and filtered. The filtrate was concentrated in vacuo. The residual oil was subjected to chromatogra-

phy on silica gel, eluting with CHCl$_3$–MeOH (95:5), to give the title compound as yellow dense oil (101 mg, 0.37 mmol, 26% yield). ^{1}H NMR (CDCl$_3$, 400 MHz) δ 0.85 (t, $J = 7.3$ Hz, 3H), 1.47 (q, $J = 7.6$ Hz, 2H), 1.57 (dq, $J = 4.2$ Hz, 10.7 Hz, 2H), 2.05–2.18 (m, 4H), 2.28 (t, $J = 7.8$ Hz, 2H), 2.87 (t, $J = 12.2$ Hz, 2H), 3.38–3.50 (m, 1H), 6.71 (d, $J = 7.6$ Hz, 1H), 7.22 (d, $J = 8.1$ Hz, 1H), 7.37 (t, $J = 7.8$ Hz, 1H), 7.46 (d, $J = 6.1$ Hz, 1H), 8.39 (d, $J = 5.9$ Hz, 1H), 9.07 (s, 1H). MS (ESI) m/z 268 (M$-$1)$^-$.

12.9.54. *N*1-(5-Isoquinolyl)-*N*4-propyl-1,4-cyclohexane-diamine (22c).

To a mixture of 1,4-cyclohexane mono-ethyleneketal (6.20 g, 40 mmol), 5-aminoisoquinoline (4.33 g, 30 mmol), and acetic acid (0.5 mL) in MeOH (50 mL) was added BH$_3$–pyridine complex (4.0 mL, 40 mmol) dropwise at 0 °C. The mixture was stirred at rt for 18 h and concentrated for removal of MeOH. The residue was dissolved in 50% acetic acid (50 mL). The solution was stirred at 80 °C for 3 h and concentrated for removal of AcOH. The mixture was basified by the addition of saturated NaHCO$_3$ aq. The aqueous layer was extracted with CHCl$_3$. The CHCl$_3$ layer was dried over anhydrous Na$_2$SO$_4$ and filtered. The filtrate was concentrated in vacuo. The residual oil was subjected to chromatography on silica gel, eluting with CHCl$_3$, to give 4-(5-isoquinolylamino)-1-cyclohexanone (5.80 g, 24 mmol).

To a mixture of 4-(5-isoquinolylamino)-1-cyclohexa-none (60 mg, 0.25 mmol), propylamine (52 mg, 0.5 mmol) in MeOH (1 mL), NaBH(OAc)$_3$ (111 mg, 0.5 mmol) was added dropwise at 0 °C. The reaction mixture was stirred at rt for 18 h and quenched by addition of saturated NaHCO$_3$ aq. The aqueous layer was extracted with CHCl$_3$. The CHCl$_3$ layer was dried over anhydrous Na$_2$SO$_4$ and filtered. The filtrate was concentrated in vacuo. The residual oil was subjected to a reverse phase HPLC (ODS), eluting with 5% TFA aq–acetonitrile (4:1), to give the title compound as yellow dense oil (18 mg, *syn*-isomer; 22 mg, *anti*-isomer). *anti*-Isomer: ^{1}H NMR (CDCl$_3$, 400 MHz) δ 0.87 (t, $J = 7.4$ Hz, 3H), 1.18–1.32 (m, 4H), 1.41–1.52 (m, 2H), 1.94–2.06 (m, 2H), 2.14–2.16 (m, 2H), 2.44–2.58 (m, 1H), 2.57 (t, $J = 7.5$ Hz, 2H), 3.31–3.44 (m, 1H), 4.06–4.20 (m, 1H), 6.70 (d, $J = 7.6$ Hz, 1H), 7.21 (d, $J = 8.0$ Hz, 1H), 7.38 (t, $J = 7.7$ Hz, 1H), 7.44 (t, $J = 6.1$ Hz, 1H), 8.38 (t, $J = 5.9$ Hz, 1H), 9.07 (s, 1H). MS (ESI) m/z 284 (M+1)$^+$. *syn*-Isomer: ^{1}H NMR (CDCl$_3$, 400 MHz) δ 0.86 (t, $J = 7.3$ Hz, 3H), 1.40–1.50 (m, 2H), 1.50–1.60 (m, 2H), 1.68–1.76 (m, 4H), 1.80–1.90 (m, 2H), 2.57 (t, $J = 7.3$ Hz, 2H), 2.58–2.68 (m, 1H), 3.60–3.70 (m, 1H), 4.33–4.45 (m, 1H), 6.68 (d, $J = 7.8$ Hz, 1H), 7.20 (d, $J = 7.6$ Hz, 1H), 7.36 (t, $J = 7.7$ Hz, 1H), 7.47 (t, $J = 5.8$ Hz, 1H), 8.37 (t, $J = 6.1$ Hz, 1H), 9.07 (s, 1H). MS (ESI) m/z 284 (M+1)$^+$.

12.9.55. *N*1-(5-Isoquinolyl)-*N*4-methyl-1,4-cyclohexan-ediamine (22d).

Compound **22d** was prepared from methylamine/MeOH solution in a manner similar to

that described for **22c** with a yield of 69%, as yellow dense oil. A mixture of two diastereomers in a ratio of ca. 1:1. MS (ESI) m/z 256 (M+1)$^+$. ^{1}H NMR (CDCl$_3$, 400 MHz) δ 1.4–1.8 (m, 8H), 2.0–2.4 (m, 2H), 2.44 (s, 3H), 6.69 (d, $J = 7.5$ Hz, 1H), 7.3–7.6 (m, 2H), 8.35 (d, $J = 6.1$ Hz, 1H), 9.07 (br s, 1H).

12.9.56. *N*-(1-Benzyl-3-piperizyl)-*N*-(5-isoquinolyl)amine (23a).

To a solution of 3-hydroxypiperizine (10.0 g, 100 mmol) in 3 M NaOH aq (100 mL) was added a solution of di-*tert*-butyl dicarbonate (25.0 g, 120 mmol) in THF (100 mL) dropwise at 0 °C. The reaction mixture was stirred at rt for 1 h and evaporated for removal of THF. The remaining aqueous layer was extracted with EtOAc. The EtOAc layer was dried over anhydrous Na$_2$SO$_4$ and filtered. The filtrate was concentrated in vacuo. To a mixture of the residue and triethylamine (20 mL) in anhydrous DMSO (100 mL) was added sulfur trioxide–trimethylamine complex (44.4 g, 200 mmol) portionwise at 0 °C. The reaction mixture was stirred at rt for 18 h and quenched by addition of saturated NaHCO$_3$ aq. The aqueous layer was extracted with EtOAc. The EtOAc layer was dried over anhydrous Na$_2$SO$_4$ and filtered. The filtrate was concentrated in vacuo. The crude mixture was purified by silica gel column chromatography (CHCl$_3$) to give the interme-diate, 3-(*tert*-butyloxycarbonyl)piperizinone (15.6 g). To a mixture of the intermediate (3.7 g, 20 mmol), 5-am-inoisoquinoline (2.5 g, 17 mmol), and anhydrous Na$_2$SO$_4$ (14.2 g, 100 mmol) in AcOH (100 mL), sodium triacetoxyborohydride (4.5 g, 20 mmol) was added dropwise at 0 °C. The reaction mixture was stirred at rt for 18 h and evaporated for removal of AcOH. The resulting mixture was basified by saturated NaHCO$_3$ aq. The aqueous layer was extracted with EtOAc. The EtOAc layer was dried over anhydrous Na$_2$SO$_4$ and filtered. The filtrate was concentrated in vacuo. The residual oil was subjected to chromatography on silica gel, eluted with CHCl$_3$–MeOH (95:5), to give *tert*-butyl 3-(5-isoquinolylamino)-1-piperizinecarboxylate as a yellow dense oil (3.7 g, 12 mmol, 60% yield in three steps).

To a solution of *tert*-butyl 3-(5-isoquinolylamino)-1-piperizinecarboxylate (66 mg, 0.20 mmol) in CHCl$_3$ (1 mL) was added trifluoroacetic acid (1 mL) dropwise at rt. The resulting mixture was stirred at rt for 3 h and concentrated in vacuo. To a mixture of residue and K$_2$CO$_3$ (69 mg, 0.50 mmol) in CH$_3$CN (1 mL) was added a solution of 4-chlorobenzylchloride (40 mg, 0.25 mmol) in CH$_3$CN (0.5 mL) dropwise at 0 °C. The reaction mixture was stirred at rt for 18 h and quenched by addition of water. The aqueous layer was extracted with EtOAc. The EtOAc layer was dried over anhydrous Na$_2$SO$_4$ and filtered. The filtrate was concentrated in vacuo. The residual oil was subjected to chromatogra-phy on silica gel, eluted with CHCl$_3$–MeOH (95:5), to give the title compound as yellow dense oil (18 mg, 0.057 mmol, 29% yield in this step). ^{1}H NMR (CDCl$_3$, 400 MHz) δ 1.40–2.05 (m, 5H), 2.25–2.98 (m, 3H), 3.37–4.10 (m, 3H), 6.65–6.80 (m, 1H), 7.24–7.58 (m, 8H), 8.47

(d, $J = 5.9$ Hz, 1H), 9.12 (s, 1H). MS (ESI) m/z 318 $(M+1)^+$.

12.9.57. N-[1-(4-Methylpentyl)-3-piperidyl]-N-(5-isoquinolyl)amine (23b).

A mixture of 3-hydroxypiperidine (1.0 g, 9.9 mmol), 1-bromo-4-methylpentane (1.65 g, 10 mmol), and K_2CO_3 (2.76 g) in DMF (10 mL) was stirred for 12 h and quenched by addition of water. The aqueous layer was extracted with EtOAc. The organic layer was washed with saturated aqueous NaCl, dried over anhydrous Na_2SO_4, filtered, and concentrated in vacuo to give N-(4-methyl)pentane-3-hyroxypiperidine (2.04 g, 11 mmol). To a mixture of the compound, N-(4-methyl)pentane-3-hyroxypiperidine (760 mg, 4 mmol) and 5-aminoisoquinoline (473 mg, 3.3 mmol) in Ti(O-i-Pr)$_4$ was added a solution of sodium borohydride (77.6 mg, 2.3 mmol) suspended in MeOH (3.8 mL). The reaction mixture was stirred for 18 h and quenched by addition of water. The reaction mixture was extracted with EtOAc. The EtOAc layer was washed with saturated NaCl aq, dried over anhydrous Na_2SO_4, filtered, and concentrated in vacuo. The crude mixture was purified by silica gel column chromatography, eluting by CHCl$_3$–MeOH to give the title compound (17.4 mg, 2% yield) as yellow dense oil. ^{1}H NMR (CDCl$_3$, 400 MHz) δ 0.88–0.91 (m, 1H), 0.90 (dd, $J = 6.6$ Hz, 6H), 1.25 (m, 2H), 1.55 (m, 4H), 1.76 (br s, 2H), 2.36 (m, 4H), 2.53 (br s, 1H), 2.69 (br s, 1H), 3.79 (s, 1H), 6.77 (d, $J = 7.9$ Hz, 1H), 7.26 (d, $J = 7.9$ Hz, 1H), 7.44 (d, $J = 7.9$ Hz, 1H), 7.57 (d, $J = 6.0$ Hz, 1H), 8.45 (d, $J = 6.0$ Hz, 1H), 9.14 (s, 1H). MS (ESI) m/z 312 $(M+1)^+$.

12.9.58. N-(4-Acetylphenyl)-N′-(5-isoquinolyl)urea (24a).

To a solution of 4-amino-isoquinoline (100 mg, 0.69 mmol) in toluene (2 mL) was added 4-acetylphenyl-isocyanate (123 mg, 0.76 mmol) at rt. The reaction mixture was stirred at 110 °C for 3 h and diluted with ether. The resulting precipitate was collected by filtration, washed with ether, and dried up in vacuo to give the title compound as a colorless solid. ^{1}H NMR (CD$_3$OD, 400 MHz) δ 2.48 (s, 3H), 7.5–7.6 (m, 3H), 7.8–7.9 (m, 4H), 8.12 (d, $J = 5.0$ Hz, 1H), 8.39 (d, $J = 5.0$ Hz, 1H), 9.16 (s, 1H). MS (ESI) m/z 306 $(M+1)^+$.

12.9.59. N-(2,6-Dichlorophenyl)-N′-(5-isoquinolyl)urea (24b), and N-(2,4,6-trichlorophenyl)-N′-(5-isoquinolyl)urea (24c).

Compound 24b and 24c were prepared from 2,6-dichloroisocyanate or 2,4,6-trichloroisocyanate in a manner similar to that described for the compound 24a with a yield of about 75%. 24b: ^{1}H NMR (CDCl$_3$, 400 MHz) δ 7.3–7.4 (m, 3H), 7.57 (dd, $J = 7.7$ Hz, 1H), 7.75 (d, $J = 5.9$ Hz, 1H), 7.81 (d, $J = 7.7$ Hz, 1H), 7.98 (d, $J = 7.7$ Hz, 1H), 8.51 (d, $J = 5.9$ Hz, 1H), 9.20 (s, 1H). MS (ESI) m/z 331 $(M-1)^-$. 24c: ^{1}H NMR (CDCl$_3$, 400 MHz) δ 7.43 (m, 1H), 7.51 (m, 1H), 7.60 (d, $J = 6.0$ Hz, 1H), 7.6–7.8 (m, 2H), 8.47 (d, $J = 6.0$ Hz, 1H), 9.18 (s, 1H). MS (ESI) m/z 365 $(M-1)^-$.

12.9.60. N-(2,6-Difluorobenzyl)-N′-(5-isoquinolyl)urea (25a).

To a mixture of 2,6-difluorophenylacetic acid (86 mg, 0.50 mmol) and triethylamine (0.4 mL) in toluene (2 mL) was added diphenylphosphoryl azide (165 mg, 0.60 mmol) dropwise at rt. The reaction mixture was stirred at 110 °C for 1 h followed by addition of 5-aminoisoquinoline (65 mg, 0.45 mmol) and successively DMF (0.2 mL). The resulting mixture was stirred at 110 °C for 3 h and diluted with EtOAc and water. The resulting precipitate was filtered and dried up in vacuo to give the title compound (85 mg, 0.27 mmol, 54% yield) as a colorless solid. Mp 196–197 °C. ^{1}H NMR (CDCl$_3$, 400 MHz) δ 4.69 (s, 2H), 7.21 (dd, $J = 7.4$ Hz, 8.8 Hz, 1H), 7.35 (d, $J = 8.0$ Hz, 1H), 7.55 (t, $J = 7.9$ Hz, 1H), 7.75 (dd, $J = 6.4$ Hz, 8.3 Hz, 1H), 8.04 (d, $J = 7.6$ Hz, 1H), 8.31 (d, $J = 6.1$ Hz, 1H), 9.10 (s, 1H). MS (ESI) m/z 314 $(M+1)^+$.

12.9.61. N-(2,6-Dichlorobenzyl)-N′-(5-isoquinolyl)urea (25b).

Compound 25b was prepared from 2,6-dichlorophenylacetic acid in a manner similar to that described for the compound 25a with a yield of 52%, as a colorless solid. Mp 215–220 °C. ^{1}H NMR (CDCl$_3$, 400 MHz) δ 4.75 (s, 2H), 6.90 (t, $J = 8.0$ Hz, 2H), 7.26 (tt, $J = 6.5$ Hz, 8.5 Hz, 1H), 7.54 (t, $J = 7.9$ Hz, 1H), 7.75 (t, $J = 8.3$ Hz, 2H), 7.99 (d, $J = 7.8$ Hz, 1H), 8.31 (d, $J = 6.1$ Hz, 1H), 9.10 (s, 1H). MS (ESI) m/z 347 $(M+1)^+$.

12.9.62. N-[1-(4-Fluoro-1-benzyl)-4-piperidylmethyl]-N-(5-isoquinolyl)amine (26).

To a mixture of 4-piperidinemethnol (345 mg, 3.0 mmol) and K_2CO_3 (414 mg, 3.2 mmol) in acetonitrile (2 mL) was added a solution of 4-fluorobenzylchloride (432 mg, 3.0 mmol) in acetonitrile (2 mL) dropwise at 0 °C. The reaction mixture was stirred at rt for 5 h and diluted with EtOAc. The mixture was filtered through Celite. The filtrate was concentrated in vacuo. To the residue, triethylamine (0.5 mL) in anhydrous DMSO (2 mL) and sulfur trioxide–trimethylamine complex (700 mg, 5 mmol) was added portionwise at 0 °C. The reaction mixture was stirred at rt for 18 h and quenched by addition of saturated NaHCO$_3$ aq. The aqueous layer was extracted with EtOAc. The EtOAc layer was dried over anhydrous Na_2SO_4 and filtered. The filtrate was concentrated in vacuo. To the residue, 5-aminoisoquinoline (288 mg, 2.0 mmol) in MeOH (3 mL) was added followed by addition of NaBH(OAc)$_3$ (666 mg, 3.0 mmol) at 0 °C. The reaction mixture was stirred at rt for 18 h and quenched by addition of saturated NaHCO$_3$ aq. The aqueous layer was extracted with CHCl$_3$. The CHCl$_3$ layer was dried over anhydrous Na_2SO_4 and filtered. The filtrate was concentrated in vacuo. The residual oil was subjected to chromatography on silica gel, eluting with CHCl$_3$–MeOH (95:5), to give the title compound as yellow dense oil (439 mg, 0.087 mmol, 44%). ^{1}H NMR (CDCl$_3$, 400 MHz) δ 1.82 (br t, $J = 11.2$ Hz, 2H), 1.95–2.05 (m, 2H), 2.14 (br t, $J = 11.2$ Hz, 2H), 2.45–2.52 (m, 1H), 2.95 (br d, $J = 11.6$ Hz, 2H), 3.43 (s, 2H), 3.51 (s, 2H), 6.85–7.02 (m, 2H), 7.01 (d, $J = 4.6$ Hz, 1H), 7.25–7.37 (m, 2H), 7.78 (d, $J = 4.2$ Hz, 1H), 7.95 (dd, $J = 1.5$ Hz,

4.0 Hz, 1H), 8.07 (d, *J* = 2.6 Hz, 1H), 8.24 (d, *J* = 2.6 Hz, 1H), 8.40 (dd, *J* = 1.5 Hz, 4.0 Hz, 1H). MS (ESI) *m/z* 350 (M+1)⁺.

12.9.63. *N*-[1-(4-Fluoro-1-benzyl)-3-piperidylmethyl]-*N*-(5-isoquinolyl)amine (27).
Compound **27** was prepared from 3-piperidinemethnol in a manner similar to that described for **26** with a yield of 45%, as yellow dense oil ¹H NMR (CDCl₃, 400 MHz) δ 1.40–1.80 (m, 3H),1.91–1.98 (m, 1H), 1.14 (br t, *J* = 4.6 Hz, 1H), 2.25 (br t, *J* = 10.4 Hz, 1H), 2.44 (br s, 1H), 2.72 (br s, 1H), 2.99 (br d, *J* = 10.0 Hz, 1H), 3.45 (d, *J* = 3.2 Hz, 2H), 3.49 (s, 2H), 6.90–7.01 (m, 2H), 7.03 (d, *J* = 4.8 Hz, 1H), 7.22–7.28 (m, 2H), 7.79 (d, *J* = 4.0 Hz, 1H), 7.99 (dd, *J* = 1.4 Hz, 3.6 Hz, 1H), 8.07 (d, *J* = 2.8 Hz, 1H), 8.24 (d, *J* = 2.4 Hz, 1H), 8.40 (dd, *J* = 1.4 Hz, 3.6 Hz, 1H). MS (ESI) *m/z* 350 (M+1)⁺.

12.9.64. *N*-(4-*tert*-Butyl-phenyl)-*N*-(5-isoquinolyl)amine (28).
5-Aminoisoquinoline (54 mg, 0.4 mmol) was dissolved in a mixture of triethylamine (0.5 mL) and DMF (2 mL). To the solution, 4-*tert*-butylphenylbronic acid (180 mg, 1.0 mmol) and cupric acetate (250 mg, 1.4 mmol) was added and stirred at rt for 3 days. The reaction mixture was filtered through Celite and diluted with water. The aqueous layer was extracted with EtOAc. The AcOEt layer was washed with water and saturated NaCl aq, dried over anhydrous Na₂SO₄, filtered, and concentrated. Purification by silica gel column chromatography eluted with hexane–EtOAc (9:1) yielded the title compound (6.5 mg, 6% yield). ¹H NMR (CDCl₃, 400 MHz) δ 1.33 (s, 9H), 5.96 (s, 1H), 7.03 (d, *J* = 8.5 Hz, 2H), 7.33 (d, *J* = 8.5 Hz, 2H), 7.47–7.49 (m, 2H), 7.57 (m, 1H), 7.76 (d, *J* = 6.1 Hz, 1H), 8.51 (d, *J* = 5.9 Hz, 1H), 9.23 (s, 1H). MS (ESI) *m/z* 277 (M+1)⁺.

12.9.65. *N*-Benzyl-*N'*-(1,3-dioxo-2,3-dihydro-1*H*-5-isoindolyl)urea (29a).
4-Aminophthalimide (80 mg, 0.5 mmol) was dissolved in toluene (1 mL) and trace amount of DMF. Benzylisocyanate (66 mg, 0.5 mmol) was added and stirred at 110 °C for 2.5 h. Water and EtOAc were added to the reaction mixture. The resulting precipitate was collected by filtration, and washed with EtOAc to give the title compound (96 mg, 66% yield) as a colorless solid. Mp > 280 °C. ¹H NMR (CDCl₃, 400 MHz) δ 4.33 (d, *J* = 4.4 Hz, 2H), 6.90 (t, *J* = 6.0 Hz, 1H), 7.22–7.35 (m, 5H), 7.61 (dd, *J* = 1.8 Hz, 8.2 Hz, 1H), 7.67 (d, *J* = 8.3 Hz, 1H), 8.02 (dd, *J* = 0.5 Hz, 2.0 Hz, 1H), 9.30 (s, 1H), 11.08 (s, 1H). MS (ESI) *m/z* 294 (M−1)⁻.

12.9.66. *N*-(2-Chlorobenzyl)-*N'*-(1,3-dioxo-2,3-dihydro-1*H*-5-isoindolyl)urea (29b).
To a mixture of 2-chlorophenylacetic acid (85 mg, 0.5 mmol) and triethylamine (61 mg, 0.6 mmol) in toluene (2 mL) was added diphenylphosphorylazide (165 mg, 0.6 mmol). The reaction mixture was stirred at 110 °C for 1 h and followed by addition of 4-aminophthalimide (81 mg, 0.5 mmol) and

DMF (2 drops). The mixture was stirred at 110 °C for 2 h and diluted with water and EtOAc. The resulting precipitate was collected by filtration and washed with EtOAc to give the title compound (37 mg, 23% yield) as a colorless solid. Mp > 280 °C. ¹H NMR (CDCl₃, 400 MHz) δ 4.40 (d, *J* = 5.6 Hz, 2H), 6.94 (t, *J* = 6.0 Hz, 1H), 7.28–7.38 (m, 2H), 7.41 (dd, *J* = 1.7, 7.6 Hz, 1H), 7.46 (dd, *J* = 1.7 Hz, 7.6 Hz, 1H), 7.61 (dd, *J* = 1.8 Hz, 8.2 Hz, 1H), 7.68 (d, *J* = 8.5 Hz, 1H), 8.01 (d, *J* = 1.5 Hz, 1H), 9.42 (s, 1H), 11.08 (s, 1H). MS (ESI) *m/z* 328 (M−1)⁻.

12.9.67. *N*-(2,6-Dichlorobenzyl)-*N'*-(1,3-dioxo-2,3-dihydro-1*H*-5-isoindolyl)urea (29c).
Compound **29c** was prepared from 2,6-dichlorophenylacetic acid in a manner similar to that described for **29b** with a yield of 67% as a colorless solid. Mp 281 °C (dp). ¹H NMR (CDCl₃, 400 MHz) δ 4.60 (d, *J* = 5.4 Hz, 2H), 6.78 (t, *J* = 5.4 Hz, 1H), 7.39 (d, *J* = 7.3 Hz, 1H), 7.51 (d, *J* = 7.8 Hz, 2H), 7.55 (dd, *J* = 2.0 Hz, 8.3 Hz, 1H), 7.67 (d, *J* = 8.3 Hz, 1H), 8.01 (d, *J* = 2.0 Hz, 1H), 9.14 (s, 1H), 11.1 (s, 1H). MS (ESI) *m/z* 363 (M−1)⁻. Anal. Calcd for C₁₆H₁₁Cl₂N₃O₃: C, 52.77; H, 3.04; N, 11.54. Found: C, 52.62; H, 3.49; N, 11.25.

12.9.68. *N*-(2,6-Dichlorobenzyl)-*N'*-(6-chloro-1,3-dioxo-2,3-dihydro-1*H*-5-isoindolyl)urea (29d).
Compound **29d** was prepared from 4-amino-5-chlorophthalimide and 2,6-dichlorophenylacetic acid in a manner similar to that described for **29b** with a yield of 4% as a colorless solid. Mp > 280 °C. ¹H NMR (CDCl₃, 400 MHz) δ 4.60–4.64 (m, 2H), 7.36–7.46 (m, 3H), 7.54 (d, *J* = 7.8 Hz, 2H), 7.87 (s, 1H), 8.71 (s, 1H), 11.28 (s, 1H). MS (ESI) *m/z* 397 (M−1)⁻.

12.9.69. *O*-(2,6-Dichlorobenzyl)-*N*-(1,3-dioxo-2,3-dihydro-1*H*-5-isoindolyl)carbamate (29e).
To a mixture of 4-aminophthalimide (81 mg, 0.50 mmol) and triethylamine (0.25 mL) in CHCl₃ (1 mL) was added a solution of triphosgen (148 mg, 0.50 mmol) in CHCl₃ (1 mL) dropwise at rt. The mixture was stirred at rt for 30 min and followed by addition of 2,6-dichlorobenzylalcohol (89 mg, 0.50 mmol) portionwise at rt. The reaction mixture was stirred at rt for 18 h and quenched by addition of saturated NaHCO₃ aq. The aqueous layer was extracted with CHCl₃. The CHCl₃ layer was dried over anhydrous Na₂SO₄ and filtered. The filtrate was concentrated in vacuo. The residual oil was subjected to chromatography on silica gel, eluting with CHCl₃–MeOH (95:5), to give the title compound as a colorless solid (42 mg, 0.12 mmol, 24% yield). Mp 257–260 °C. ¹H NMR (DMSO, 400 MHz) δ 3.30 (s, 2H), 6.38 (br s, 1H), 6.78 (d, *J* = 12.2 Hz, 1H), 6.85 (s, 1H), 6.94–7.02 (m, 1H), 7.37 (d, *J* = 13.0 Hz, 1H), 7.44 (d, *J* = 12.2 Hz, 1H). MS (ESI) *m/z* 365 (M+1)⁺.

12.9.70. 2-(2,6-Dichlorophenoxy)-*N*-(1,3-dioxo-2,3-dihydro-1*H*-5-isoindolyl)acetamide (29f).
To a mixture of 2,6-dichlorophenol (1.0 g, 6.13 mmol) and K₂CO₃

(1.02 g, 7.36 mmol) in acetonitrile (8 mL) was added methylbromoacetate (1.12 g, 6.75 mmol). The reaction mixture was stirred at 80 °C for 3 h and quenched by addition of water. The aqueous layer was extracted with EtOAc. The EtOAc layer was washed with saturated aqueous NaCl, dried over Na_2SO_4, filtered, and solvent was removed in vacuo. The residue was purified by silica gel column chromatography ($CHCl_3$) to give 2,6-dichlorophenoxyacetic acid ethyl ester. A mixture of the compound in 5% NaOH aq (10 mL) and EtOH (10 mL) was stirred at 80 °C for 1 h. The reaction mixture was concentrated, acidified to pH 4 with 5% HCl aq, and extracted with EtOAc. The EtOAc layer was washed with saturated NaCl aq, dried over anhydrous Na_2SO_4, and concentrated in vacuo to give 2, 6-dichlorophenoxyacetic acid (1.08 g, 79%) as a colorless solid.

To a solution of the acetic acid (150 mg, 0.68 mmol) and 4-aminophthalimide (100 mg, 0.62 mmol) in DMF (2 mL) was added WSC–HCl (147 mg, 0.74 mmol) and HOBt–H_2O (100 mg, 0.74 mmol). The reaction mixture was stirred at rt for 4 h and quenched by addition of water. The aqueous layer was extracted with EtOAc. The EtOAc layer was washed with saturated NaCl aq, dried over anhydrous Na_2SO_4, filtered, and concentrated. Purification was carried out by silica gel column chromatography ($CHCl_3$–MeOH 95:5). The title compound (64 mg, 28% yield) was obtained as colorless solid. Mp > 280 °C. ^{1}H NMR ($CDCl_3$, 400 MHz) δ 4.71 (s, 2H), 7.24 (t, $J = 8.5$ Hz, 1H), 7.54 (d, $J = 8.1$ Hz, 1H), 7.54 (d, $J = 8.1$ Hz, 1H), 7.80 (d, $J = 8.3$ Hz, 1H), 8.02 (dd, $J = 2.0$ Hz, 8.1 Hz, 1H), 8.24 (d, $J = 2.0$ Hz, 1H), 10.70 (s, 1H), 11.25 (s, 1H). MS (ESI) m/z 365 $(M+1)^+$.

12.9.71. N-(1,3-Dioxo-2,3-dihydro-1H-5-isoindolyl)-N'-propylurea (30a).
To a solution of 4-aminophthalimide (80 mg, 0.5 mmol) in toluene (1 mL) and a trace amount of DMF, n-propylisocyanate (42 mg, 0.5 mmol) was added and stirred at 110 °C for 2.5 h. Water was added to the reaction mixture and extracted with EtOAc. The EtOAc layer was washed with saturated NaCl aq, dried over anhydrous Na_2SO_4, concentrated, and purified by preparative TLC ($CHCl_3$–acetone 95:5) to give the title compound (35 mg, 29% yield) as a colorless solid. Mp > 280 °C. ^{1}H NMR ($CDCl_3$, 400 MHz) δ 0.88 (t, $J = 7.4$ Hz, 3H), 1.41–1.51 (m, 2H), 3.07 (q, $J = 6.8$ Hz, 2H), 6.40 (t, $J = 5.6$ Hz, 1H), 7.58 (dd, $J = 2.1$ Hz, 8.2 Hz, 1H), 7.66 (d, $J = 8.3$ Hz, 1H), 8.00 (d, $J = 1.7$ Hz, 1H), 9.14 (s, 1H), 11.06 (s, 1H). MS (ESI) m/z 246 $(M-1)^-$.

12.9.72. N-(1,3-Dioxo-2,3-dihydro-1H-5-isoindolyl)-N'-phenylurea (30b).
To a solution of 4-aminophthalimide (80 mg, 0.5 mmol) in toluene (1 mL) was added phenylisocyanate (59 mg, 0.5 mmol) and DMF (1 drop). The reaction mixture was stirred at 110 °C for 2.5 h. Water and EtOAc was added to the reaction mixture. The precipitated crystal was collected by filtration and washed with EtOAc to give the title compound (95 mg, 68% yield) as a colorless solid. Mp > 280 °C. ^{1}H NMR

($CDCl_3$, 400 MHz) δ 7.01 (t, $J = 7.3$ Hz, 1H), 7.31 (t, $J = 7.9$ Hz, 2H), 7.48 (dd, $J = 1.0$ Hz, 8.5 Hz, 2H), 7.67 (dd, $J = 1.8$ Hz, 8.2 Hz, 1H), 7.73 (d, $J = 8.3$ Hz, 1H), 8.05 (d, $J = 1.5$ Hz, 1H), 8.89 (s, 1H), 9.36 (s, 1H), 11.14 (s, 1H). MS (ESI) m/z 280 $(M-1)^-$.

12.9.73. N-(1,3-Dioxo-2,3-dihydro-1H-5-isoindolyl)-N'-(2,6-dichlorophenyl)urea (30c).
Compound 30c was prepared from 4-amino-5-chlorophthalimide and 2,6-dichlorophenylacetic acid in a manner similar to that described for 30b with a yield of 86% as a colorless solid. Mp > 280 °C. ^{1}H NMR ($CDCl_3$, 400 MHz) δ 7.35 (dd, $J = 7.8$ Hz, 8.0 Hz, 1H), 7.60 (d, $J = 8.1$ Hz, 2H), 7.72 (d, $J = 1.2$ Hz, 2H), 8.04 (d, $J = 1.2$ Hz, 1H), 8.50 (s, 1H), 9.69 (s, 1H), 11.13 (s, 1H). MS (ESI) m/z 349 $(M-1)^-$.

12.9.74. N-(1,3-Dioxo-2,3-dihydro-1H-5-isoindolyl)-N'-(4-methylpiperizyl)urea (30d).
To a mixture of 4-amino-1H-phthlimide (200 mg, 1.23 mmol) and triethylamine (1.5 mL) in $CHCl_3$ (5 mL) was added a solution of triphosgen (366 mg, 1.23 mmol) in $CHCl_3$ (1 mL) dropwise at rt. The resulting mixture was stirred at rt for 30 min and followed by addition of 1-amino-4-methylpiperazine (142 mg, 1.23 mmol) portionwise at rt. The reaction mixture was stirred at rt for 18 h and diluted by water. The resulting precipitate was collected by filtration, washed with ether, and dried up in vacuo to give the title compound as a colorless solid. ^{1}H NMR ($CDCl_3$, 400 MHz) δ 1.8–2.0 (m, 2H), 2.2–2.3 (m, 2H), 2.8–2.9 (m, 2H), 3.0–3.1 (m, 2H), 3.42 (br s, 3H), 7.50 (m, 1H), 7.65 (m, 1H), 7.72 (br s, 1H). MS (ESI) m/z 302 $(M-1)^-$.

12.9.75. N-(1-Benzylpiperidin-4-yl)-N'-(1,3-dioxo-2,3-dihydro-1H-5-isoindolyl)urea (30e).
Compound 30e was prepared from 1-benzyl-4-aminopiperizine in a manner similar to that described for 30d. ^{1}H NMR (CD_3OD, 400 MHz) δ 1.4–1.5 (m, 2H), 1.9–2.0 (m, 2H), 2.0–2.1 (m, 2H), 2.7–2.8 (m, 2H), 3.5–3.6 (m, 3H), 5.05 (br s, 2H), 7.2–7.3 (m, 5H), 7.53 (dd, $J = 8.1$ Hz, 2.0 Hz, 1H), 7.59 (d, $J = 8.1$ Hz, 1H), 7.88 (d, $J = 2.0$ Hz, 1H). MS (ESI) m/z 377 $(M-1)^-$.

12.9.76. 4-{[(2,6-Dichloroanilino)carbonyl]amino}benzamide (31).
To a solution of 4-aminobenzdiamide (100 mg, 0.73 mmol) in toluene (1 mL) was added 2,6-dichloro-phenylisocyanate (138 mg, 0.73 mmol). The reaction mixture was stirred at 110 °C for 2 h and diluted with water and EtOAc. The precipitate was collected by filtration and washed with EtOAc to give the title compound (210 mg, 88% yield) as a colorless solid. Mp > 280 °C. ^{1}H NMR ($CDCl_3$, 400 MHz) δ 7.15 (br s, 1H), 7.31 (t, $J = 8.1$ Hz, 1H), 7.49 (d, $J = 8.8$ Hz, 2H), 7.52 (d, $J = 8.1$ Hz, 2H), 7.79 (d, $J = 8.8$ Hz, 2H), 7.87 (br s 1H), 8.31 (br s, 1H), 9.22 (br s, 1H). MS (ESI) m/z 323 $(M-1)^-$.

Acknowledgements

References and notes

1. Matsui, T.; Amano, M.; Yamamoto, T.; Chihara, K.; Nakafuku, M.; Ito, M.; Nakano, T.; Okawa, K.; Iwamatsu, A.; Kaibuchi, K. *EMBO J.* **1996**, *15*, 2208.
2. Ishizaki, T.; Maekawa, M.; Fujisawa, K.; Okawa, K.; Iwamatsu, A.; Fujita, A.; Watanabe, N.; Saito, Y.; Kakizuka, A.; Morii, N.; Narumiya, S. *EMBO J.* **1996**, *15*, 1885.
3. Fukata, Y.; Amano, M.; Kaibuchi, K. *Trends Pharmacol. Sci.* **2001**, *22*, 32.
4. Kawano, Y.; Fukata, Y.; Oshiro, N.; Amano, M.; Nakamura, T.; Ito, M.; Matsumura, F.; Inagaki, M.; Kaibuchi, K. *J. Cell Biol.* **1999**, *147*, 1023.
5. Kimura, K.; Ito, M.; Amano, M.; Chihara, K.; Fukata, Y.; Nakafuku, M.; Yamamori, B.; Feng, J.; Nakano, T.; Okawa, K.; Iwamatsu, A.; Kaibuchi, K. *Science* **1996**, *273*, 245.
6. Uehata, M.; Ishizaki, T.; Satoh, H.; Ono, T.; Kawahara, T.; Morishita, T.; Tamakawa, H.; Yamagami, K.; Inui, J.; Maekawa, M.; Narumiya, S. *Nature* **1997**, *389*, 990.
7. (a) Riento, K.; Ridley, A. J. *Nat. Rev. Mol. Cell. Biol.* **2003**, *4*, 446; (b) Zhou, Y.; Su, Y.; Baolin, L.; Ryder, J. W.; Xin, W.; Gonzalez-DeWhitt, P. A.; Gelfanova, V.; Hale, J. E.; May, P. C.; Paul, S. M.; Binhui, N. *Science* **2003**, *302*, 1215.
8. Itoh, K.; Yoshioka, K.; Akedo, H.; Uehata, M.; Ishizaki, T.; Narumiya, S. *Nature Med.* **1999**, *5*, 221.
9. Lipinski, C. A.; Lombardo, F.; Dominy, B. W.; Feeney, P. J. *Adv. Drug Delivery Rev.* **1997**, *23*, 3.
10. Suzuki, Y.; Yamamoto, M.; Wada, H.; Ito, M.; Nakano, T.; Sasaki, Y.; Narumiya, S.; Shiku, H.; Nishikawa, M. *Blood* **1999**, *93*, 3408.
11. Berman, H. M.; Westbrook, J.; Feng, Z.; Gilliland, G.; Bhat, T. N.; Weissig, H.; Shindyalov, I. N.; Bourne, P. E. *Nucleic Acids Res.* **2000**, *28*, 235.
12. Engh, R. A.; Girod, A.; Kinzel, V.; Huber, R.; Bossemeyer, D. *J. Biol. Chem.* **1996**, *271*, 26157.
13. Needleman, S.; Wunsch, C. *J. Mol. Biol.* **1970**, *48*, 443.
14. Schulze-Gahmen, U.; Brandsen, J.; Jones, H. D.; Morgan, D. O.; Meijer, L.; Vesely, J.; Kim, S. H. *Proteins* **1995**, *22*, 378.
15. Hubbard, S. R.; Wei, L.; Ellis, L.; Hendrickson, W. A. *Nature* **1994**, *372*, 746.
16. SYBYL software package, Tripos Inc., 1699 South Hanley Rd., St. Louis, MO 63144, USA. FlexiDock used in this study was one included in the version 6.5 package.
17. Prade, L.; Engh, R. A.; Girod, A.; Kinzel, V.; Huber, R.; Bossemeyer, D. *Structure* **1997**, *5*, 1627.
18. Nagar, B.; Bornmann, W. G.; Pellicena, P.; Schindler, T.; Veach, D. R.; Miller, W. T.; Clarkson, B.; Kuriyan, J. *Cancer Res.* **2002**, *62*, 4236.
19. Amano, M.; Chihara, K.; Nakamura, N.; Kaneko, T.; Matsuura, Y.; Kaibuchi, K. *J. Biol. Chem.* **1999**, *274*, 32418.
20. Ishizaki, T.; Uehata, M.; Tamechika, I.; Keel, J.; Nonomura, K.; Maekawa, M.; Narumiya, S. *Mol. Pharmacol.* **2000**, *57*, 976.
21. (a) Kubota, M.; Ohba, S. *Acta Crystallogr. Sect. B, Struct. Sci.* **1992**, *48*, 849; (b) Gao, Q.; Jeffery, G. A.; Ruble, J. R.; McMullan, R. K. *Acta Crystallogr., Sect. B, Struct. Sci.* **1991**, *47*, 742; (c) Kuroda, R.; Wilman, D. E. V. *Acta Crystallogr. Sect. C, Cryst. Struct. Commun.* **1985**, *41*, 1543.
22. Amono, M.; Ito, M.; Kimura, K.; Fukata, Y.; Chihara, K.; Nakano, T.; Matuura, Y.; Kaibuchi, K. *J. Biol. Chem.* **1996**, *271*, 20246.
23. Sekimata, M.; Tsujimura, K.; Tanaka, J.; Takeuchi, Y.; Inagaki, N.; Inagaki, M. *J. Cell. Biol.* **1996**, *132*, 635–641.
24. Lovell, S. C.; Davis, I. W.; Arendall, W. B., III; de Bakker, P. I.; Word, J. M.; Prisant, M. G.; Richardson, J. S.; Richardson, D. C. *Proteins* **2003**, *50*, 437.
25. Cornell, W. D.; Cieplak, P.; Bayly, C. I.; Gould, I. R.; Kenneth, M.; Merz, K. M.; Ferguson, D., Jr.; David, M.; Spellmeyer, C.; Fox, T.; Caldwell, J. W.; Kollman, A. P. *J. Am. Chem. Soc.* **1995**, *117*, 5179.
26. Exner, T. E.; Keil, M.; Moeckel, G.; Brickmann, J. *J. Mol. Mod.* **1998**, *4*, 340.
27. Swärd, K.; Dreja, K.; Susnjar, M.; Hellstrand, P.; Hartshorne, D. J.; Walsh, M. P. *J. Physiol.* **2000**, *522*, 33.
28. (a) Gaßel, M.; Breitenlechner, C. B.; Ruger, P.; Jucknischke, U.; Schneider, T.; Huber, R.; Bossemeyer, D.; Engh, R. A. *J. Mol. Biol.* **2003**, *329*, 1021; (b) Breitenlechner, C.; Gaßel, M.; Hidaka, H.; Kinzel, V.; Huber, R.; Engh, R. A.; Bossemeyer, D. *Structure* **2003**, *11*, 1595.